RSC Advances

PAPER

View Article Online
View Journal | View Issue

Cite this: *RSC Adv.*, 2021, **11**, 26241

Design, synthesis and mechanistic study of new benzenesulfonamide derivatives as anticancer and antimicrobial agents *via* carbonic anhydrase IX inhibition†

Mohamed T. M. Nemr,[a] Asmaa M. AboulMagd,[b] Hossam M. Hassan,[*cd] Ahmed A. Hamed,[e] Mohamed I. A. Hamed[f] and Mohamed T. Elsaadi[gh]

Changes in gene expression cause uncontrolled cell proliferation and consequently tumor hypoxia. The tumor cells shift their metabolism to anaerobic glycolysis with a significant modification in pH. Therefore, an over expression of carbonic anhydrase IX (CA IX) genes was detected in many solid tumors. Accordingly, selective inhibition of CA IX can be a useful target for discovering novel antiproliferative agents. The present study described the synthesis of new aryl thiazolone–benzenesulfonamides **4a–j** as well as their carbonic anhydrase IX inhibitory effect. All the designed derivatives were evaluated for their anti-proliferative activity against triple-negative breast cancer cell line (as MDA-MB-231) and another breast cancer cell line (MCF-7) in addition to normal breast cell line MCF-10A. Compounds **4b–c**, **4e**, **4g–h** showed significant inhibitory effect against both cancer cell lines at concentration ranges from 1.52–6.31 μM, with a high selectivity against breast cancer cell lines ranges from 5.5 to 17.5 times. Moreover, three sulfonamides derivatives **4e**, **4g** and **4h** showed excellent enzyme inhibition against CA IX with IC_{50} 10.93–25.06 nM and against CA II with IC_{50} 1.55–3.92 μM that revealed their remarkable selectivity for CA IX over CA II. Additionally, **4e** was able to induce apoptosis in MDA-MB-231 with a significant increase in the annexin V-FITC percent by 22 fold as compared with control. Cellular uptake on MDA-MB-231 cell lines were carried out using HPLC method on the three active compounds (**4e**, **4g** and **4h**). On the other hand inhibition of one or more CAs present in bacteria was reported to interfere with bacterial growth. So, the new benzenesulfonamides were evaluated against their antibacterial and anti-biofilm activities. Analogues **4e**, **4g** and **4h** exhibited significant inhibition at 50 μg mL^{-1} concentration with 80.69%, 69.74% and 68.30% against *S. aureus* compared to the positive control CIP which was 99.2%, while compounds **4g** and **4h** showed potential anti-biofilm inhibition 79.46% and 77.52% against *K. pneumonia*. Furthermore, the designed compounds were docked into CA IX (human) protein (PDB ID: 5FL6) and molecular modeling studies revealed favorable binding interactions for the active inhibitors. Finally, the predictive ADMET studies showed that, compounds **4e**, **4g** and **4h** possessed promising pharmacokinetic properties.

Received 8th July 2021
Accepted 26th July 2021

DOI: 10.1039/d1ra05277b

rsc.li/rsc-advances

1 Introduction

Cancer remains one of the leading causes of death worldwide, thus necessitating the development of novel and effective therapies. Although modern therapeutic agents have been developed over the past 100 years, the successful treatment of cancer appears to be a powerful challenge at the start of the present century. This challenge lies in the difficulty to discover novel selective agents that inhibit the proliferation of tumor cells without being toxic to normal cells.[1–4] According to GLOBOCAN, 2020 estimation, about 19.3 million cancer cases and 10 million cancer deaths are estimated to occur worldwide in 2020. Breast cancer (BC) is one of the most commonly diagnosed and the second leading cause of cancer related deaths in

[a]*Pharmaceutical Organic Chemistry Department, Faculty of Pharmacy, Cairo University, Kasr El-Eini street 11562, Cairo, Egypt*
[b]*Pharmaceutical Chemistry Department, Faculty of Pharmacy, Nahda University, Beni-Suef 62513, Egypt*
[c]*Pharmacognosy Department, Faculty of Pharmacy, Beni-Suef University, Beni-Suef 62513, Egypt. E-mail: hossam.mokhtar@nub.edu.eg*
[d]*Pharmacognosy Department, Faculty of Pharmacy, Nahda University, Beni-Suef 62513, Egypt*
[e]*Microbial Chemistry Department, National Research Center, Giza, Egypt*
[f]*Organic and Medicinal Chemistry Department, Faculty of Pharmacy, Fayoum University, Fayoum 63514, Egypt*
[g]*Pharmaceutical Chemistry Department, Faculty of Pharmacy, Beni-Suef University, Beni-Suef 62513, Egypt*
[h]*Pharmaceutical Chemistry Department, Faculty of Pharmacy, Sinai University, Egypt*
† Electronic supplementary information (ESI) available. See DOI: 10.1039/d1ra05277b

females. Also, BC represents 1 in 4 cancer cases diagnosed among women globally.[5] It is often characterized by hypoxia regions due to poor vascularization.[6] Moreover, BC cells that survive in this adverse media are found to be resistant to radiotherapy and chemotherapy.[7] Among the genes that contributes to hypoxic condition production and the adaptation of hypoxic tumor cells are carbonic anhydrase IX (CA IX) and XII (CA XII).[8] CA IX is reported to be overexpressed in various tumor entities, especially in those with invasive BC, immunohistochemical CA IX over expression is consistent with worse relapse-free and overall survival.[9] Knowing the topology of carbonic anhydrase active site offers a promising strategy for developing selective inhibitors. This mammalian CAs active site is characterized by a cone-shaped cavity with two preserved environments, known as hydrophobic and hydrophilic walls, and a Zn^{2+} ion at the bottom. This Zn^{2+} ion is tetrahedrally conserved with three characteristic histidine residues namely (His94, His96, and His119) and a solvent molecule; which binds to the hydroxide ion that reacted with carbon dioxide to yield bicarbonate.[10,11] As a result, CA inhibitors should have a specific zinc binding group (ZBG) that can coordinate efficiently with the Zn^{2+} ion at the binding site. Actually, ZBG binds with different chemical moieties that called the compound "tail" that enables the interactions with certain residues in the active site. One of the important mechanisms of anticancer activity of sulfonamides is the inhibition of carbonic anhydrase isozymes.[12–15] The amino thiazole based coumarin benzenesulfonamide compound **I** (Fig. 1) showed potent inhibitory activity against hCA IX with a K_i value of 25.04 nM as compared to the reference compound acetazolamide **II** which had a K_i value of 25 nM, in addition, compound **I** showed potent inhibitory activity against hCA XII when compared with AZA, with K_i values of 3.94 and 5.7 nM respectively.[16] A series of diamide-based benzenesulfonamides were synthesized and evaluated as inhibitors of the metalloenzyme CA IX, compound **III** (Fig. 1) achieved the best CA IX/I and IX/II selectivity with selective indexes (SIs) of 985 and 13.8, respectively.[17] Recently a CA IX inhibitor, **SLC-0111** (**IVa**, Fig. 1), entered in Phase I clinical trials by potentiating the cytotoxic activity of the traditional chemotherapeutic agents against MCF-7 breast cancer cells, and HCT-116 colorectal cancer cells. **SLC-0111** and some of its analogues **IVa–d** are among isoform-selective sulfonamides that are discovered as CAIs in the last period.[18–20]

4-Thiazolone and 4-thiazolidinones derivatives are important heterocyclic class possess a wide range of biological activities such as anticancer, anti-diabetic, anti-microbial, anti-viral, anti-inflammatory, and anti-convulsant.[21–23] Compounds **V–VIII** (Fig. 1) have been reported to demonstrate significant anti-tumor activity against the human BC cell line (MCF-7).[24–27]

From another point of view, it has shown that interference with the growth and/or pathogenicity of many microorganisms is affected by inhibition of CAs.[28–30] This can be explained by the participation of CAs enzymes in metabolic process control, or in the pH homeostasis, that are highly relevant in the bacteria.[31,32] Chohan, *et al.*33 introduced a series of 4-hydroxycoumarin sulfonamides derivatives and studied their *in vitro* anti-bacterial activities for different Gram-positive (*S. aureus*, *B. subtilis*) and Gram-negative (*S. flexneri*, *S. typhi*, *E. coli*, *P. aeruginosa*) bacteria. The amino substituted ethyl coumarin benzenesulfonamide derivative **IX** (Fig. 2) exhibited the best activity against *E. coli* and *S. flexenari* with a zone inhibition (ZI) value of 10 and 09 mm, respectively, as compared to the standard reference drug imipenem which had a ZI values of 30 and 27 mm, respectively. Moreover, a series of thiazole derivatives were synthesized and evaluated for their antimicrobial activity and cytotoxicity. Compound **Xa** (Fig. 2) exhibited potent cytotoxicity more effective than cisplatin ($IC_{50} = 13.7 \pm 1.2$ mg mL^{-1}) and compound **Xb** was found to be the most promising antibacterial agent against *Pseudomonas aeruginosa*.[34]

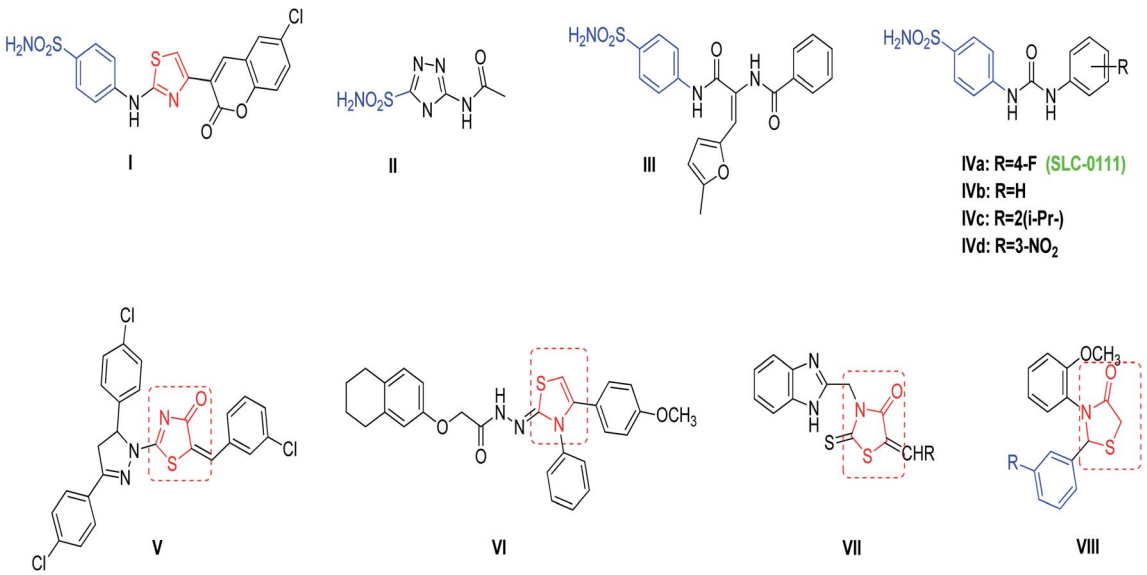

Fig. 1 Reported benzenesulfonamides-based CAIs (I–IV), thiazolone and thiazolidine derivatives (V–VIII) as anticancer agents.

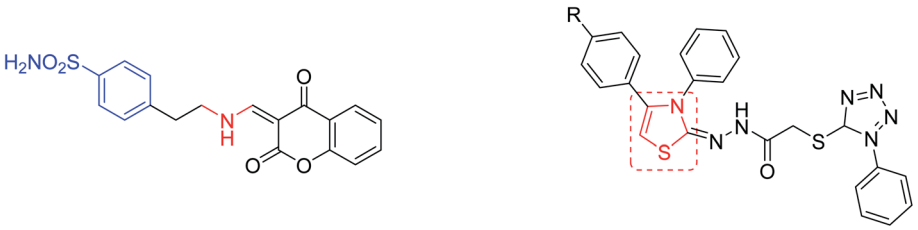

Fig. 2 Reported benzenesulfonamides-based CAIs (IX) and thiazole derivatives (Xa,b) as antibacterial agents.

From previously mentioned, subsequently, we represent the synthesis, and biological evaluation of a new series of 4-thiazolone-based benzenesulfonamides **4a–j** with the "tail approach" (Fig. 3). It is based on appending "tails", with a different chemical nature, to the aromatic or heterocyclic ring owning the zinc binding sulfonamide group, to interact with the middle and the rim parts of the active site cavity. Firstly, the bioisosteric replacement tactic was selected to replace the urea linker (compounds **SLC-0111**, Fig. 3) with the hetero 4-thiazolone that was expected to bind firmly with the active site's "spacer" region, also structural rigidification was employed to prevent the rotation and attains CA selectivity. Moreover, bioisosteric replacement was applied by using benzylidene tails incorporating different substituents to ensure appropriate SAR exploration concerning the hydrophobic region of the binding cleft.

All the newly-synthesized 4-thiazolone-based benzenesulfonamides **4a–j** were characterized and biologically for their anti-proliferative activity against breast cancer cell lines; MDA-MB-231 and MCF-7 in addition to normal breast cell line MCF-10A. Moreover, all the newly synthesized compounds were evaluated for their selective CA IX inhibitory effect to CA II, to gain insight and further explain the mechanism of the dual activity of the prepared hybrid structure as anticancer and antimicrobial agents. The most active derivative **5e** was further examined for its apoptosis induction potential in MDA-MB-231 cells. Finally, docking study was performed to explore the affinity of the synthesized derivatives against CA IX in addition to ADMET profile to predict their pharmacokinetic properties.

2 Experimental

2.1 Chemistry

Melting points are uncorrected and have been measured on a Stuart melting point apparatus (Stuart Scientific, Redhill, UK). On the Shimadzu IR 435 spectrophotometer, the IR spectra (KBr) were calculated and values are shown in cm^{-1}. Using a Varian Gemini 300-BB spectrophotometer, the ^{1}H-NMR (400 MHz) and ^{13}C-NMR (100 MHz) spectra were carried out (Bruker, Munich, Germany), using tetramethylsilane TMS as internal standard. Splitting patterns have been designated as follows: s: singlet; d: doublet; t: triplet; m: multiplet and chemical shift values are reported in ppm on δ scale. Progress of the reactions was tracked by TLC using TLC sheets precoated with Merck 60 F 254 UV florescent silica gel and visualized them using UV lamps. The chemicals used are supplied by Across from (New Jersey, USA). At the Microanalytical Center, Al-Azhar University, elemental analyses were performed.

2.1.1 Synthesis of 2-chloro-*N*-(4-sulfamoylphenyl)-acetamide 2.[35] A suspension of sulfanilamide **1** (1.72 gm, 0.01 mol) in acetone, K_2CO_3 (2.76 g, 0.02 mol) was added. To this mixture, 2-chloroacetyl chloride (1.354 g, 0.012 mol) was added drop-wise. The reaction mixture was allowed to be stirred at 0 °C for 1 h then left to cool at room temperature. TLC was used to monitor the reaction until completion. The reaction mixture was filtered and the filtrate was evaporated *in vacuo* to yield the crude solid. The precipitate was washed with water several times and crystallized from ethanol to give white product of compound **2**.

2.1.2 Synthesis of ((4-*oxo*-4,5-dihydrothiazol-2-yl)amino) benzenesulfonamide 3.[36] To a solution of 2-chloro-*N*-(4-

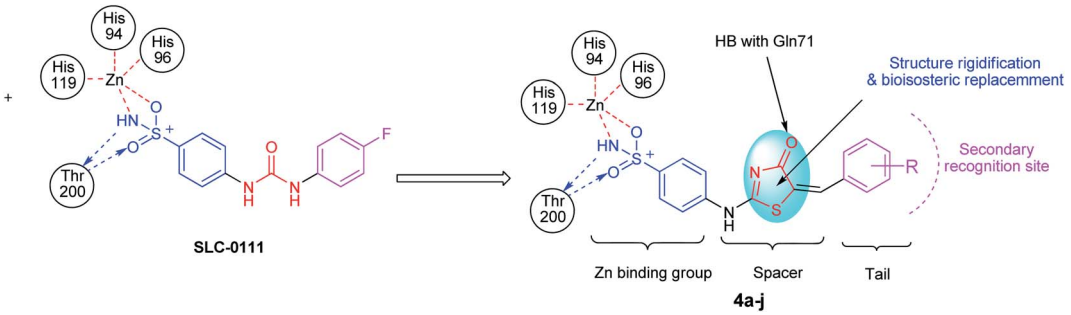

Fig. 3 The design strategy for the new thiazolone–sulfonamide conjugates as selective hCA IX inhibitors.

sulfamoylphenyl) acetamide **2** (2.625 g, 0.01 mol) in absolute ethanol (20 mL) ammonium thiocyanate (0.76 g, 0.01 mol) was added. The whole mixture was refluxed for 3 h and the reaction was monitored using TLC. The obtained solid during reflux was filtered and washed with water. The precipitate was crystallized from ethanol to yield white crystals of compound **3**.

Yield 70%, m.p. 250–252 °C as reported.

2.1.3 General procedure for the synthesis of compounds 4a–j. To a solution of ((4-*oxo*-4,5-dihydrothiazol-2-yl)amino) benzenesulfonamide **3** (0.271 g, 0.001 mol) in glacial acetic acid (20 mL), sodium acetate (0.164 g, 0.002 mol) and the appropriate aldehyde (0.02 mol) were added. The whole mixture was refluxed for 24 h for derivatives **3a–d** and 48 h for derivatives **3e–j** and the reaction was monitored by TLC until completion of the reaction. The solid resulted was filtered and washed from ethanol several times. The precipitate was crystallized from acetic acid to afford compounds **4a–j**.

*2.1.3.1 (E)-4-(5-Benzylidene-4-oxo-4,5-dihydrothiazol-2-ylamino)benzenesulfonamide **4a**.* Creamy solid: yield, 84%; m.p. 326 ± 2 °C; IR (KBr) ν_{max}: 3313, 3284 (NH_2), 3201 (NH), 2978 (CH aliph.), 1678 (C=O) cm^{-1}, ^{1}H-NMR (DMSO-d_6) δ: 7.02 (d, J = 8.0 Hz, 1H, Ar-H), 7.35 (s, 1H, CH), 7.42–7.64 (m, 5H, Ar-H), 7.68 (d, J = 8.0 Hz, 2H, Ar-H), 7.83 (d, J = 8.0 Hz, 1H, Ar-H), 8.00 (s, 2H, NH_2), 12.35 (s, 1H, NH) ppm. MS (M_w: 359.04): *m*/*z* 360.94 (M + 2, 66.32%), 359.18 (43.74%), 329.61 (86.59%), 267.29 (100%); anal. calcd. For $C_{16}H_{13}N_3O_3S_2$: C, 53.47; H, 3.65; N, 11.69. Found: C, 53.69; H, 3.91; N, 11.28% as reported.[37]

*2.1.3.2 (E)-4-(5-(4-Hydroxybenzylidene)-4-oxo-4,5-dihydrothiazol-2-ylamino)benzenesulfonamide **4b**.* Yellow solid: yield, 87%; m.p. 234 ± 2 °C; IR (KBr) ν_{max}: 3441 (OH), 3348, 3255 (NH_2), 3201 (NH), 2951 (CH aliph.), 1670 (C=O) cm^{-1}, ^{1}H-NMR (DMSO-d_6) δ: 6.87 (d, J = 8.0 Hz, 1H, Ar-H), 6.95 (d, J = 8.0 Hz, 1H, Ar-H), 7.35 (s, 1H, CH), 7.49–7.58 (m, 3H, Ar-H), 7.65 (d, J = 8.0 Hz, 1H, Ar-H), 7.84 (d, J = 8.0 Hz, 1H, Ar-H), 7.91 (s, 1H, NH), 7.96 (d, J = 8.0 Hz, 1H, Ar-H), 10.41 (s, 2H, NH_2), 12.17 (s, 1H, OH) ppm. ^{13}C-NMR (DMSO-d_6) δ: 116.8, 117.0, 117.1, 122.0, 124.4, 127.0, 127.7, 129.2, 132.5, 133.2, 134.4, 140.4, 144.9, 160.0, 165.6, 167.4 ppm. MS (M_w: 375.03): *m*/*z* 375.47 (M^+, 23.67%), 344.80 (66.80%), 314.23 (49.20%), 300.56 (100%); anal. calcd. For $C_{16}H_{13}N_3O_4S_2$: C, 51.19; H, 3.49; N, 11.19. Found: C, 50.97; H, 3.63; N, 11.45% as reported.[37]

*2.1.3.3 (E)-4-(5-(4-Methoxybenzylidene)-4-oxo-4,5-dihydrothiazol-2-ylamino)benzenesulfonamide **4c**.* Light brown solid: yield, 85%; m.p. 345 ± 2 °C; IR (KBr) ν_{max}), 3329, 3251 (NH_2), 3201 (NH), 2978 (CH aliph.), 1678 (C=O) cm^{-1}, ^{1}H-NMR (DMSO-d_6) δ: 3.87 (s, 3H, OCH_3), 7.05 (d, J = 8.0 Hz, 1H, Ar-H), 7.13 (d, J = 8.0 Hz, 1H, Ar-H), 7.18 (d, J = 8.0 Hz, 1H, Ar-H), 7.36 (s, 1H, CH), 7.46 (d, J = 8.0 Hz, 2H, Ar-H), 7.60 (d, J = 8.0 Hz, 2H, Ar-H), 7.84 (s, 2H, NH_2), 7.95 (d, J = 8.0 Hz, 1H, Ar-H), 12.14 (s, 1H, NH) ppm. ^{13}C-NMR (DMSO-d_6) δ: 55.9, 115.4, 115.6, 120.8, 122.0, 125.9, 127.0, 127.1, 129.2, 132.2, 132.8, 133.9, 140.5, 144.9, 161.2, 161.8, 165.5 ppm. MS (M_w: 389.05): *m*/*z* 391.67 (M + 2, 16.26%), 389.82 (M^+, 50.15%), 369.60 (81.39%), 283.86 (48.96%), 149.28 (100%); anal. calcd. For $C_{17}H_{15}N_3O_4S_2$: C, 52.43; H, 3.88; N, 10.79. Found: C, 52.66; H, 4.05; N, 11.08%.

*2.1.3.4 (E)-4-(5-(4-Chlorobenzylidene)-4-oxo-4,5-dihydrothiazol-2-ylamino)benzenesulfonamide **4d**.* Yellow solid: yield, 81%; m.p. 314 ± 2 °C; IR (KBr) ν_{max}), 3383, 3325 (NH_2), 3251 (NH), 2978 (CH aliph.), 1674 (C=O) cm^{-1}, ^{1}H-NMR (DMSO-d_6) δ: 7.19 (d, J = 8.0 Hz, 1H, Ar-H), 7.38 (s, 1H, CH), 7.51 (d, J = 8.0 Hz, 2H, Ar-H), 7.65 (d, J = 8.0 Hz, 1H, Ar-H), 7.70 (d, J = 8.0 Hz, 2H, Ar-H), 7.83 (d, J = 8.0 Hz, 1H, Ar-H), 7.95 (s, 2H, NH_2), 8.00 (d, J = 8.0 Hz, 1H, Ar-H), 12.14 (s, 1H, NH) ppm. ^{13}C-NMR (DMSO-d_6) δ: 121.2, 122.0, 122.7, 127.0, 127.8, 129.2, 129.8, 130.0, 131.8, 132.3, 132.4, 135.0, 136.0, 140.9, 145.0, 167.2 ppm. MS (M_w: 393.00): *m*/*z* 394.78 (M + 2, 13.37%), 393.55 (M^+, 39.40%), 389.85 (59.83%), 350.38 (62.60%), 236.22 (55.85%), 110.01 (100%); anal. calcd. For $C_{16}H_{12}ClN_3O_3S_2$: C, 48.79; H, 3.07; N, 10.67. Found: C, 48.95; H, 3.20; N, 10.51%.

2.1.3.5 Synthesis of 5-allyl-2-hydroxy-3-methoxybenzaldehyde. $POCl_3$ (0.1 mol) was added portion wise to DMF (10 mL) and stirred at room temperature for 30 minutes. Then, a solution of eugenol (0.1 mol) in DMF (1 mL) was added portion wise at room temperature. The whole mixture was stirred for 24 h and then poured onto ice (10 g). The product was neutralized with 40% NaOH and the resultant oil was separated and purified using column chromatography starting with petroleum to afford the 5-allyl-2-hydroxy-3-methoxybenzaldehyde.

*2.1.3.6 (E)-4-(5-(5-Allyl-2-hydroxy-3-methoxybenzylidene)-4-oxo-4,5-dihydrothiazol-2-ylamino)benzenesulfonamide **4e**.* Light brown solid: yield, 79%; m.p. 259 ± 2 °C; IR (KBr) ν_{max}), 3523 (OH), 3360, 3271 (NH_2), 3201 (NH), 2862 (CH aliph.), 1678 (C=O) cm^{-1}, ^{1}H-NMR (DMSO-d_6) δ: 3.74 (d, J = 5.6 Hz, 2H, $\underline{CH_2}$–CH=CH_2), 4.04 (s, 3H, OCH_3), 5.08 (d, J = 8.2 Hz, 2H, CH_2–CH=$\underline{CH_2}$), 5.90 (m, 1H, CH_2–$\underline{CH}$=CH_2), 7.11 (d, J = 8.0 Hz, 1H, Ar-H), 7.22 (d, J = 8.0 Hz, 1H, Ar-H), 7.31 (s, 1H, CH), 7.46 (d, J = 8.0 Hz, 2H, Ar-H), 7.74 (d, J = 8.0 Hz, 2H, Ar-H), 7.80 (s, 2H, NH_2), 7.95 (s, 1H, NH), 11.42 (s, 1H, OH) ppm. ^{13}C-NMR (DMSO-d_6) δ: 40.6, 58.4, 113.7, 112.7, 118.9, 121.8, 127.0, 127.5, 129.0, 130.2, 136.5, 140.1, 152.9, 157.1, 171.6, 172.4, 186.9 ppm. MS (M_w: 445.08): *m*/*z* 446.92 (M + 1, 9.33%), 413.56 (15.47%), 392.77 (61.79%), 388.09 (32.24%), 360.87 (17.87%), 326.78 (100%), 130.70 (51.36%); anal. calcd. For $C_{20}H_{19}N_3O_5S_2$: C, 53.92; H, 4.30; N, 9.43. Found: C, 54.09; H, 3.87; N, 9.34%.

*2.1.3.7 (E)-4-((4-oxo-2-(4-Sulfamoylphenylamino)thiazol-5(4H)-ylidene)methyl)benzoic acid **4f**.* White solid: yield, 69%; m.p. 245 ± 2 °C; IR (KBr) ν_{max}) 3518 (OH), 3344, 3255 (NH_2), 3197 (NH), 2854 (CH aliph.), 1766, 1678 (2C=O) cm^{-1}, ^{1}H-NMR (DMSO-d_6) δ: 5.52 (s, 1H, OH), 7.16 (d, J = 8.0 Hz, 1H, Ar-H), 7.32 (s, 1H, CH), 7.48 (m, 2H, Ar-H), 7.64 (d, J = 8.0 Hz, 1H, Ar-H), 7.82 (m, 3H, Ar-H), 7.86 (s, 2H, NH_2), 7.96 (d, J = 8.0 Hz, 1H, Ar-H), 8.27 (s, 1H, NH) ppm. ^{13}C-NMR (DMSO-d_6) δ: 110.8, 122.0, 125.6, 127.7, 128.5, 130.0, 130.6, 131.4, 132.9, 140.5, 151.2, 168.2, 193.5 ppm. MS (M_w: 403.03): *m*/*z* 403.72 (M^+, 23.08%), 394.62 (42.22%), 355.00 (67.74%), 320.27 (100%); anal. calcd. For $C_{17}H_{13}N_3O_5S_2$: C, 50.61; H, 3.25; N, 10.42. Found: C, 50.85; H, 3.41; N, 10.33%.

*2.1.3.8 (E)-4-(5-(4-Nitrobenzylidene)-4-oxo-4,5-dihydrothiazol-2-ylamino)benzenesulfonamide **4g**.* Yellow solid: yield, 77%; m.p. 317 ± 2 °C; IR (KBr) ν_{max}) 3417, 3314 (NH_2), 3232 (NH), 2897 (CH aliph.), 1651 (C=O) cm^{-1}, ^{1}H-NMR (DMSO-d_6) δ: 7.20 (d, J = 8 Hz, 1H, Ar-H), 7.35 (d, J = 8 Hz, 1H, Ar-H), 7.42 (s, 1H, CH), 7.51 (d, 2H, Ar-H), 7.77 (m, 4H, Ar-H), 7.98 (s, 2H, NH_2), 8.02 (s, 1H, NH) ppm. MS (M_w: 404.02): *m*/*z* 404.38 (M^+, 61.70%), 399.81

(24.26%), 351.23 (65.60%), 344.38 (67.88%), 218.86 (100%); anal. calcd. For $C_{16}H_{12}N_4O_5S_2$: C, 47.52; H, 2.99; N, 13.85. Found: C, 47.68; H, 3.15; N, 14.02%.

2.1.3.9 (E)-4-(5-(4-Hydroxy-3-methoxybenzylidene)-4-oxo-4,5-dihydrothiazol-2-ylamino)benzenesulfonamide ***4h***. Orange solid: yield, 82%; m.p. 263 ± 2 °C; IR (KBr) ν_{max}) 3561 (OH), 3360, 3271 (NH_2), 3201 (NH), 2862 (CH aliph.), 1678 (C=O) cm^{-1}, ^{1}H-NMR (DMSO-d_6) δ: 4.04 (s, 3H, OCH_3), 6.95 (d, J = 8.0 Hz, 1H, Ar-H), 7.35 (s, 1H, CH), 7.38 (m, 3H, Ar-H), 7.50 (s, 1H, OH), 7.55 (d, J = 8.0 Hz, 1H, Ar-H), 7.65 (d, J = 8.0 Hz, 1H, Ar-H), 7.84 (d, J = 8.0 Hz, 1H, Ar-H), 7.92 (s, 1H, NH), 7.99 (s, 2H, NH_2) ppm. ^{13}C-NMR (DMSO-d_6) δ: 57.0, 116.8, 117.0, 117.2, 122.0, 124.4, 127.0, 127.5, 129.1, 132.5, 133.2, 134.5, 136.4, 140.3, 144.9, 160.0, 160.8 ppm. MS (M_w: 405.05): m/z 405.44 (M^+, 58.86%), 476.91 (47.73%), 352.81 (96.34%), 329.33 (61.38%), 284.90 (100%); anal. calcd. For $C_{17}H_{15}N_3O_5S_2$: C, 50.36; H, 3.73; N, 10.36. Found: C, 50.22; H, 3.94; N, 10.54%.

2.1.3.10 (E)-4-(4-oxo-5-(3,4,5-Trimethoxybenzylidene)-4,5-dihydrothiazol-2-ylamino)benzenesulfonamide ***4i***. Yellow solid: yield, 71%; m.p. 275 ± 2 °C; IR (KBr) ν_{max}) 3367, 3297 (NH_2), 3255 (NH), 2839 (CH aliph.), 1681 (C=O) cm^{-1}, ^{1}H-NMR (DMSO-d_6) δ: 3.72 (s, 3H, OCH_3), 3.86 (s, 6H, OCH_3), 7.05 (d, J = 8.0 Hz, 2H, Ar-H), 7.35 (s, 1H, CH), 7.50 (s, 1H, NH), 7.67 (d, J = 8.0 Hz, 1H, Ar-H), 7.85 (d, 2H, J = 8.0 Hz, Ar-H), 7.96 (d, J = 8.0 Hz, 1H, Ar-H), 8.00 (s, 2H, NH_2) ppm. ^{13}C-NMR (DMSO-d_6) δ: 56.6, 60.7, 105.8, 108.2, 110.4, 112.6, 120.7, 127.1, 128.9, 129.2, 134.1, 136.2, 140.3, 145.0, 153.8, 159.5, 165.4, 167.2 ppm. MS (M_w: 449.07): m/z 449.36 (M^+, 48.46%), 421.11 (30.76%), 295.15 (41.02%), 268.01 (40.96%), 183.35 (100%); anal. calcd. For $C_{19}H_{19}N_3O_6S_2$: C, 50.77; H, 4.26; N, 9.35. Found: C, 51.03; H, 4.42; N, 9.47%.

2.1.3.11 (E)-4-(5-(4-(Dimethylamino)benzylidene)-4-oxo-4,5-dihydrothiazol-2-ylamino)benzenesulfonamide ***4j***. Pale yellow solid: yield, 83%; m.p. 333 ± 2 °C; IR (KBr) ν_{max}) 3356, 3305 (NH_2), 3251 (NH), 2819 (CH aliph.), 1670 (C=O) cm^{-1}, ^{1}H-NMR (DMSO-d_6) δ: 3.02 (s, 3H, CH_3), 3.04 (s, 3H, CH_3), 6.84 (d, J = 8.0 Hz, 1H, Ar-H), 7.34 (s, 1H, CH), 7.40 (m, 2H, Ar-H), 7.51 (d, J = 8.0 Hz, 2H, Ar-H), 7.63 (d, J = 8.0 Hz, 1H, Ar-H), 7.82 (s, 1H, NH), 7.86 (d, J = 8.0 Hz, 1H, Ar-H), 7.94 (d, J = 8.0 Hz, 1H, Ar-H), 7.99 (s, 2H, NH_2) ppm. ^{13}C-NMR (DMSO-d_6) δ: 57.0, 116.8, 117.0, 117.2, 122.0, 124.4, 127.1, 127.5, 129.1, 132.5, 133.2, 134.5, 136.4, 140.3, 144.988, 160.02, 160.75 ppm. MS (M_w: 402.08): m/z 402.86 (M^+, 72.86%), 354.24 (42.73%), 337.03 (61.34%), 323.27 (100%); anal. calcd. For $C_{18}H_{18}N_4O_3S_2$: C, 53.71; H, 4.51; N, 13.92. Found: C, 53.60; H, 4.68; N, 14.08% as reported.[37]

2.2 Biological evaluation

2.2.1 MTT cytotoxicity assay. The American Type Culture Collection is the source of cell lines used that were cultured in DMEM (obtained from Invitrogen/Life Technologies) and 10% FBS (Hyclone). Additionally, 10 μg mL^{-1} insulin (purchased from Sigma), as well as 1% penicillin–streptomycin were added. The remaining chemicals and reagents were all purchased from Sigma or Invitrogen. Plate cells with a density ranges from 1.2 to 1.8, 10 000 cells per well in a 96-well plate was evacuated to a centrifuge tube for 24 hours in a volume of 100 μL complete growth medium and 100 μL of the investigated substance per well before the MTT experiment. After that, the cell layer is rinsed with 0.25 percent (w/v) trypsin 0.53 mM EDTA solution to eliminate any traces of serum containing trypsin inhibitor. After adding 2.0 to 3.0 mL of trypsin EDTA solution to the flask, the cells were observed under an inverted microscope until the cell layer was dispersed, which normally took 5 to 15 minutes. A pipette was employed to gently aspirate cells after adding 6.0 to 8.0 mL of full growth media. The cell suspension was relocated to a another centrifuge tube containing the medium and cells from the first step to be centrifuged for 5 to 10 minutes at 125×g, with the supernatant discarded. In fresh growth medium, the cell pellet was resuspended. After that, the necessary aliquots of the cell suspension are added to fresh culture containers. After 24 hours of incubation at 37 °C, the cells were treated with serial quantities of the tested substance and incubated for 48 hours at 37 °C. After that, the plates were viewed under an inverted microscope and the MTT assay was carried out.[38] For usage with −16 multiwall plates, the MTT technique of *in vitro* cytotoxicity control is well adapted. For best results, cells should be used in the log growth process, and the final cell density should not exceed 106 cells per cm^2. Blanks should be comprised in each test to provide a full medium without cells. Take away the cultures from the incubator and place them in a sterile work environment, such as a laminar flow hood. To use, each vial of MTT [M-5655] was reconstituted with 3 mL of medium, excluding phenol red and serum. Reconstituted MTT was added to the culture medium in a volume equal to 10% of the total volume. Return the cultures to the incubator for another 2–4 hours, based on the cell type and density.

When the incubation period had ended, crops were taken from the incubator then an amount of MTT Solubilization Solution [M-8910] equivalent to the original culture's were added to the formazan crystals. In a gyratory shaker, gentle mixing is recommended to improve dissolution. Trituration may be necessary on occasion, especially in thick cultures, to guarantee that the MTT formazan crystals are completely dissolved. The absorbance is measured at wavelength 570 nm with a spectrophotometer. Background absorbance of 16 multiwall plates was measured at 690 nm and was subtracted from the 570 nm reading.[39] The concentration range used to determine IC_{50} was 100 μM, 25 μM, 6.25 μM, 1.56 μM, 0.39 μM.

2.2.2 Recovery of compounds 4e, 4h, and 4g from MDA-MB-231 for cellular uptake assay. The cell pellets were suspended in the RIPA buffer that includes 20 mM Tris/HCl at pH 8.0, 137 mM NaCl, 10% of glycerol, 5 mM EDTA, 1 mM phenylmethyl–sulfonyl fluoride, 1.5 mg of leupeptin, and protease inhibitor mixture then the cell-liquid extraction was performed. The cell extracts were subjected to centrifugation at 18 000 rpm for 15 min. 100 μg of the cell extract was each acidified by 6N HCl (1 : 1 v/v) and vortexed for 30 s. 500 μL of the extracting buffer was then added to each of the acidified cell extracts, and samples were vortexed again and shaken in the Orbited shaker (at 100 rpm) for 15 min. The upper organic layer obtained after centrifugation at 18 000 rpm for 20 min was filtered by a membrane filter. Finally this organic layer was transferred to

a clean injection HPLC sample vials of about 100 μL for quantitative analysis using HPLC.

*2.2.2.1 HPLC analysis of compounds **4e**, **4g** and **4h**.* The HPLC system used to carry out the HPLC analysis of compounds **4e**, **4g** and **4h** was a Dionex Ultimate 3000 UHPLC equipped with autosampler, quaternary solvent delivery pump and diode array detector (Germany). The software used was Chromeleon software. The stationary phase used was ZORBAX Eclipse Plus® C18 column with dimensions of (250 × 4.6 mm, 5 μm) (California, USA). A mobile phase, which was composed of methanol : water (90 : 10, v/v), was used, and the samples were each injected at an injection volume of 20 μL. Each sample was injected in triplicate and UV scanning was carried out at 254 nm.

2.2.3 *In vitro* carbonic anhydrase IX and II enzyme inhibition. To each well of enzyme control (EC), sample (S), inhibitor control (IC), solvent control (SC), and background control (BC), carbonic anhydrase IX or II assay buffer was added as 80 μL, 90 μL and 80 μL in BC, EC, and S/SC/IC, respectively. While carbonic anhydrase enzyme was added by 5 μL in each of EC and S/SC/IC. Then thoroughly combine all of the ingredients and pour into the appropriate wells. Dissolve the candidate inhibitors at 10× the highest final test concentration in the selected solvent for the screening compounds, inhibitor control, and enzyme control preparations (*e.g.* DMSO). Add 10 μL test inhibitors (S, BC) or inhibitor solvent (SC). For inhibitor control (IC), add 10 μL CA inhibitor into IC well(s), and BC well. The concentration range used to determine IC_{50} was 10 μM, 1 μM, 0.1 μM, 0.01 μM. Then incubate at room temperature (RT) for 10 min. To examine the effect of the solvent on enzyme activity, prepare a parallel well(s) as a solvent control (same as EC in presence of final solvent concentration). Every test chemical should be run with its own background control because the signal from the probe may be affected, resulting in a false negative result. 5 μL of CA Substrate should be added to the BC, EC, S, SC, and IC wells and mixed thoroughly. At room temperature, measure absorbance at 405 nm in kinetic mode for 1 hour. In the linear range of the plot, two time points (t_1 and t_2) were chosen, and the corresponding values for the absorbance (Ab_1 and Ab_2) were acquired. Calculate the slope for all samples, Δabsorbance/Δt.

$$\% \text{ Relative activity} = \Delta\text{Ab of S} \times 100$$

ΔAb of EC

$$\% \text{ Relative inhibition} = \Delta\text{Ab of EC} - \Delta\text{Ab of S} \times 100$$

ΔAb of EC

2.2.4 Cell cycle analysis. MDA-MB-231 cells were treated with the aryl thiazolone–benzenesulfonamide **4e** at its IC_{50} concentration (IC_{50} = 3.58 μM) for 24 h, after that ice-cold phosphate buffered saline (PBS) was used to wash the cells. Then, the mentioned cells were treated by gathering *via* centrifugation, and remained in ice-cold 70% (v/v) ethanol. This is followed by washing using PBS, and re-suspended with RNase (100 μg mL^{-1}). About 40 μg mL^{-1} of PI was used for staining and finally analysis was carried out *via* flow cytometry (Becton Dickinson, BD, USA). CellQuest software 5.1 (Becton Dickinson) used to calculate the cell cycle distributions.[40]

2.2.5 Annexin V-FITC apoptosis assay. Annexin V-FITC/PI apoptosis detection kit obtained from (BD Biosciences, San Jose, CA, USA) was used in the assay of the phosphatidylserine externalization following the instructions of the manufacturer, as reported previously.[41]

2.2.6 Antimicrobial activity. Five Gram-negative bacteria (*Escherichia coli* ATCC 25955, *Pseudomonas aeruginosa* ATCC 10145, *Klebsiella pneumonia*, *Proteus vulgaris*, and *Salmonella typhimurium*), two Gram-positive bacteria (*Bacillus subtilis* ATCC 6633 and *Staphylococcus aureus* NRRL B-767), one yeast (*Candida albicans* ATCC 10231) were used as test organisms and antimicrobial tests were performed as described by Ingebrigtsen *et al.*[42,43] The assay was carried out in 96-well microplates (Thermo Fisher Scientific, United States), in which each well filled with 170 μL of Mueller Hinton Broth medium, 10 μL of suspension of an actively growing (log phase) culture of test microbes and 20 μL of test compounds (final concentration of 50 μg mL^{-1}).

At 37 °C for 24 h, the plates were incubated overnight. The absorbance at 600 nm for bacteria and 340 nm for *C. albicans* was measured after incubation. Using a Spectrostar Nano Microplate Reader Albicans (BMG LABTECH GmbH, Allmendgrun, Germany). As a control, ciprofloxacin and nystatin were used.

2.2.7 Anti-biofilm activity. The procedures involved employing 96-well flat polystyrene plates and four clinical microbes including Gram-positive bacteria and Gram-negative bacteria according to method,[44,45] all of the synthesized derivatives biofilm inhibitory activity was calculated with some adaptations. 180 μL of lysogenic broth (LB broth) was poured in every well and then inoculated with 10 μL of pathogenic bacteria. Subsequently the 10 μL of samples (conc. 50 μg mL^{-1}) was added along with control bacteria. The plates were allowed to be incubated for 24 h at 37 °C then the contents in the wells were removed after incubation. This is followed by washing with 200 μL of phosphate buffer saline (PBS) pH 7.2 to remove free floating bacteria and left to dry for 1 h at a sterilized laminar flow. 200 μL of crystal violet (0.1 percent, w/v) was added per well for 1 h for staining, and the excess stain was then removed, and the plates were held for drying. In addition, dried plates were washed with 95% ethanol and the optical density was calculated using a Spectrostar Nano Microplate Reader at 570 nm optical density (BMG LABTECH GmbH, Allmendgrun, Germany).

2.2.8 Molecular modeling study. Docking studies was carried out using MOE® 2010. The target macromolecule carbonic anhydrase IX's 3D crystal structure was acquired from protein databank (PDB ID: 5FL6, resolution: 1.41 Å). The protein chain was adjusted and protonated at its reported pH and temperature of 293 K, as specified in the PDB file's Experimental section. Then the protein energy was minimized by selecting CHARMM and MMFF94 force fields. After that, the active binding site was recognized and determined for docking. Then, validation was accomplished with RMSD of 1.69 Å. ChemBioDraw Ultra 12.0 was used to sketch the structures of

the designed derivatives and the ligand and were saved in MDL-SD file format. Docking studies was carried out by using Triangle matcher as placement algorithm. A maximum of 30 poses were taken into consideration for each predicted compound during the docking process. Finally, the best pose was carefully chosen consistent with its binding free energy and binding interactions within its active site.

2.2.9 ADME/Tox study. Online pkCSM was chosen to predict the pharmacokinetic properties of the designed compounds that showed potent carbonic anhydrase IX enzyme inhibition.[46] Various parameters as absorption, Lipinski's rule, water solubility, permeability to caco-2, intestinal absorption (human), permeability to skin as well as interactions with *P*-glycoprotein were measured. In this work, the findings obtained were checked against the pkCSM pharmacokinetics prediction property reference values.

2.2.10 Statistical study. Statistical analysis of cytotoxicity ad enzyme inhibition data was performed by one-way ANOVA, through GraphPad Prism software.

3 Results and discussion

3.1 Chemistry

The design in this study is based in using **SLC-0111** as a lead compound in which its ureido moiety is replaced by thiazol-4-one heterocyclic five membered ring that integrates the thio-ureido moiety involved in the reported lead compound. In this work, the design of synthesis of benzenesulfonamide derivatives containing thiazol-4-one scaffold was shown in Scheme 1. 4-((4-*oxo*-4,5-Dihydrothiazol-2-yl)amino)benzenesulfonamide **3** was prepared *via* intramolecular cyclization rearrangement reaction of previously prepared chloroacetamide derivative **2** when treated with ammonium thiocyanate in ethanol.[23,47] Furthermore, intermediate **3** underwent coupling reaction with selected aromatic aldehydes on the active methylene group of compound **3** to afford 5-aryl-4-*oxo*-4,5-dihydrothiazol-2-ylamino)benzenesulfonamides **4a–j**. The structure of the synthesized compounds **4a–j** was confirmed by different spectral data. ^{1}H-NMR spectrum of compounds **4a–j** showed the disappearance of the characteristic dd signal corresponds to CH_2 of the thiazol-4-one ring and the appearance of the characteristic singlet signal of CH proton at 7.31–7.38 ppm. Additionally, ^{1}H-NMR spectrum revealed additional protons due to the presence of additional aromatic protons signals related to aromatic aldehydes. Moreover, ^{13}C-NMR revealed the appearance of the characteristic signal of methine carbon at 145.0–161.2 ppm in addition to additional aromatic carbons which appeared in the aromatic region corresponding to substituted aromatic aldehyde moieties.

3.2 Biological evaluation

3.2.1 *In vitro* anticancer screening. The newly synthesized compounds were screened for their cytotoxic activity against three types of human breast cancer cell lines, highly resistant breast cancer cell line MDA-MB-231, MCF-7, and the normal breast cell line MCF 10A, obtained from the American Type Culture Collection (ATCC, Rockville, MD). The results were demonstrated as IC_{50} which corresponds to growth inhibition and are submitted in (Table S1†). The results revealed that all the compounds showed significant moderate to excellent growth inhibition against breast cancer cell lines. The substitution with electron donating groups showed better inhibitory effect than those substituted with electron withdrawing effect.

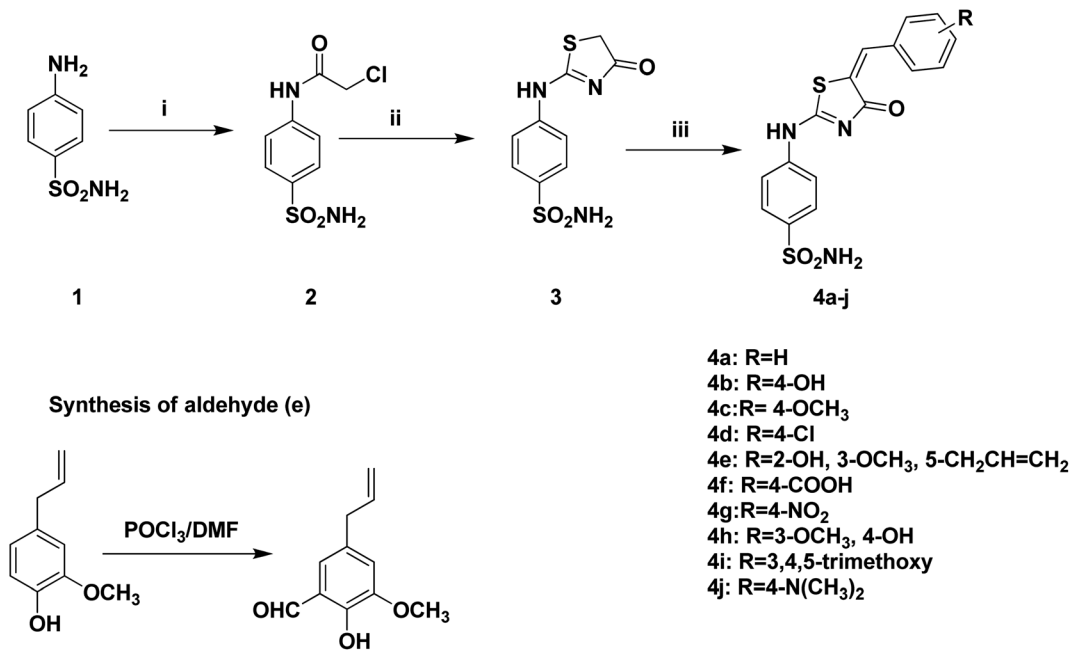

Scheme 1 Synthesis of Benzenesulfonamides compounds **4a–j**. (i) Chloroacetyl chloride, dry DMF, r.t., 2 h; (ii) ammonium thiocyanate, absolute ethanol, reflux, 1 h; (iii) appropriate aldehydes, sodium acetate, acetic acid, reflux, 24 h.

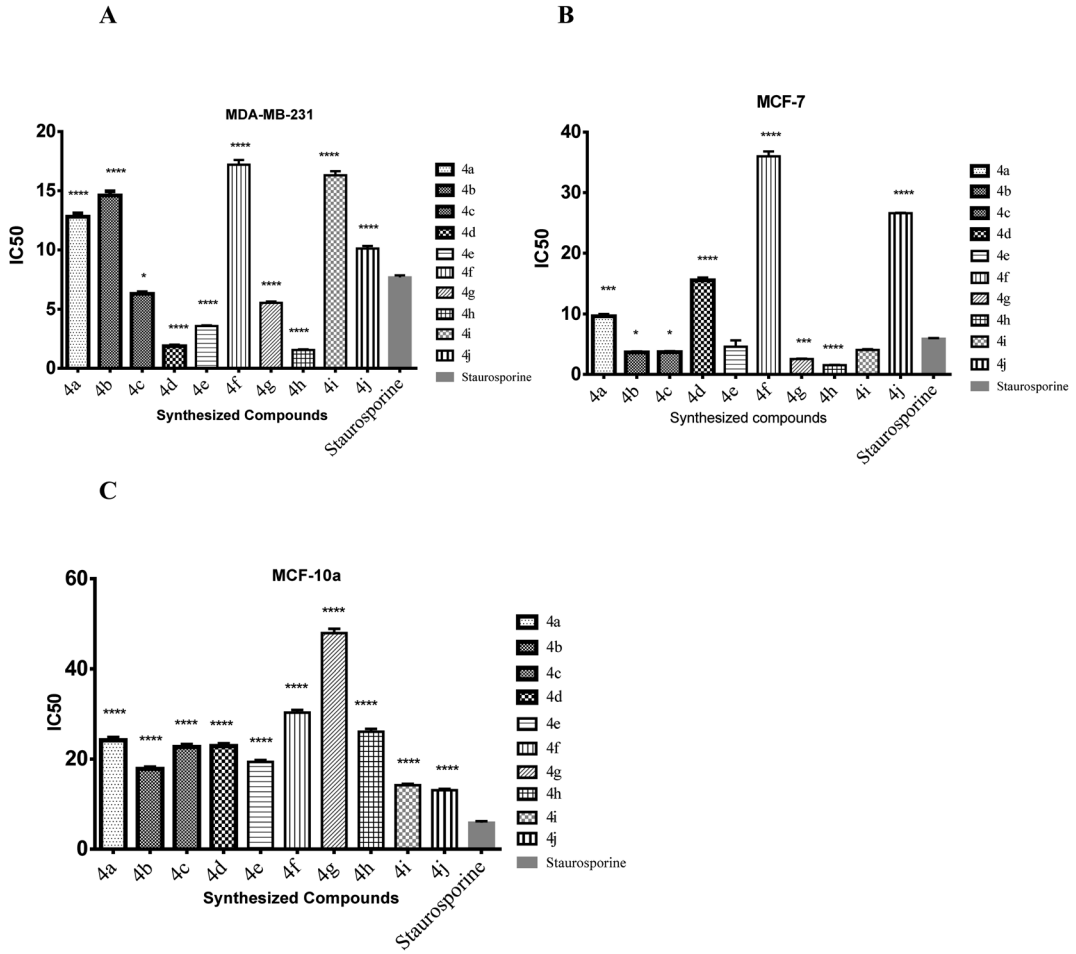

Fig. 4 The bar graphs showing the IC_{50} of the target compounds ± standard error compared to staurosporine against MDA-MB-231 cell lines. ****High significantly different from staurosporine at $p < 0.05$, ***moderate significantly different from staurosporine at $p < 0.05$. *Mild significantly different from staurosporine at $p < 0.05$.

Thus, compounds **4b** and **4c** displayed potent growth inhibition against MCF-7 with IC_{50} = 3.63 and 3.67 μM respectively compared to staurosporine (IC_{50} 5.89 μM). It is worth to mention that compound **4c** was 3.5 times more selective to MDA-MB-231 than to normal breast cell line MCF-10A (Fig. 4–6). Further analysis of the inhibitory results within the thiazol-4-one-benzenesulfonamides derivatives, compound **4e** displayed enhanced growth inhibition on both breast cancer cell lines namely MDA-MB-231 and MCF-7 (IC_{50} = 3.58 and 4.58 μM respectively) compared to staurosporine (IC_{50} 7.67 and 5.89 μM). As for its selectivity, it was found that it is selective to both breast cancer cell lines 5.5 times than MCF-10A cell line. Surprisingly, compound **4g** substituted with nitro group in the *para* position showed highly potent inhibitory effect against both breast cancer cell lines (IC_{50} = 5.54 and 2.55 μM respectively). Additionally, the *p*-nitro aryl analogue was highly selective to normal breast cell line with 8.5 times. Furthermore, the analogue (**4h**) containing vanillin tail showed the highest inhibitory activity against MDA-MB-231 and MCF-7 cell lines (IC_{50} = 1.56, and 1.52 μM respectively) with also highest selectivity 17.5 more times MCF-10A. For the trimethoxy substituted analogue (**4i**), it was found that it displayed remarkable growth inhibitory effect against MCF-7 (IC_{50} = 4.05 μM) which is more potent than staurosporine (Table 1, 4 and Fig S1†). In an attempt to clarify that compound **4e** is not the most potent

Table 1 Cytotoxic activity of the new compounds against MDA-MB-231, and MCF-7 cancer cell lines and MCF 10A normal cell line

	Cytotoxicity IC_{50} μM ± S.D.		
Compound no.	MDA-MB-231	MCF-7	MCF 10A
4a	12.8 ± 0.5	9.63 ± 0.4	24.2 ± 0.9
4b	14.6 ± 0.6	**3.63 ± 0.1**	17.8 ± 0.6
4c	**6.31 ± 0.2**	**3.67 ± 0.1**	**22.7 ± 0.8**
4d	1.88 ± 0.1	15.5 ± 0.6	22.9 ± 0.8
4e	**3.58 ± 0.1**	**4.58 ± 1.8**	**19.4 ± 0.7**
4f	17.2 ± 0.7	36 ± 1.4	30.3 ± 1.1
4g	**5.54 ± 0.2**	**2.55 ± 0.1**	**47.9 ± 1.7**
4h	**1.56 ± 0.1**	**1.52 ± 0.1**	**26.1 ± 1.1**
4i	16.3 ± 0.6	**4.05 ± 0.2**	14.2 ± 0.5
4j	10.1 ± 0.4	26.6 ± 1.0	13.1 ± 0.5
Staurosporine	7.67 ± 0.3	5.89 ± 0.2	13.0 ± 0.5

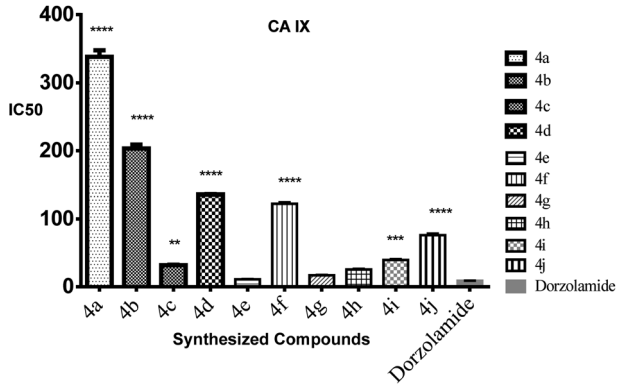

Fig. 5 The bar graphs showing the IC_{50} of the target compounds ± standard error compared to Dorzolamide against CA IX cell lines. A: ****high significantly different from dorzolamide at $p < 0.05$, ***: moderate significantly different from dorzolamide at $p < 0.05$, **: mild significantly different from dorzolamide at $p < 0.05$.

Table 2 IC_{50} of carbonic anhydrase IX and carbonic anhydrase II enzyme inhibition of derivatives **4e**, **4g** and **4h**

Compound no.	CA IX IC_{50} (μM)	CA II IC_{50} (μM)
4e	0.011	3.92
4g	0.017	1.55
4h	0.026	2.19

cytotoxic analogue yet it is most active CA IX inhibitor (Fig. 5), cellular uptake assay of compounds **4e**, **4g** and **4h** by human MDA-MB-231 cancer cells was carried out. It is interesting to note that the level of compound **4e** taken up into MDA-MB-231 cell line was 12.5 μg mL^{-1} while the intracellular amount calculated for compound **4h** was 17.07 μg mL^{-1} (Fig S2†). Comparing the cell penetration effect of the three mentioned compounds on the cytotoxic activity on MDA-MB-231 cancer cell line suggests that the potent inhibitory activity of compound **4h** could be attributed to the increased uptake of 4 h into breast cancer cell lines.

3.2.2 Carbonic anhydrase IX inhibition. The inhibitory potency of all the synthesized thiazol-4-one-benzenesulfonamide derivatives against carbonic anhydrase IX was evaluated. The results represented as IC_{50} values and are summarized in Table S1.† CA IX activity was carried out to all the synthesized compounds to determine their inhibitory abilities to decrease the reaction of hydrogenocarbonate formation and to further gain insight into structure activity relationships. Investigation of the results of CA IX inhibitory activities among the synthesized compounds revealed that the inhibitory activity ranges from 10 to 338 nM. In particular, substituent with the eugenol aldehyde was well tolerated and the best result was obtained in compound **4e** (IC_{50} = 10.93 nM). Also, among compounds with aldehydes derived from natural source, the vanillin derived analogue **4h** gave significant inhibitory activity of (IC_{50} = 25.56 nM). Moreover, compound **4g** that possess nitro group in the *para* position showed excellent inhibitory activity with IC_{50} = 16.96 nM compared to the positive control Dorzolamide (8.83 nM) and **SLC-0111** (4.5 nM) as reported[18] (Table S1† and Fig. 5). The SAR outcomes hinted that generally di-substitution and poly-substitution are more advantageous for the activity against CA IX than monosubstiution. Except for the nitro derivative, the incorporation of electron donating groups (4-OCH_3 or 4-$N(CH_3)_2$) is more beneficial for the inhibitory activity towards CA IX than electron withdrawing groups (4-Cl or 4-COOH). It was concluded from the CA IX enzyme inhibition results that compound **4e** was relatively similar in potency to benzensulfonamide derivative **III** (IC_{50} = 8.3 nM) that was reported by Abdelrahman *et al.*[17] and also had a better inhibitory activity than the other related analogues reported by them.

3.2.3 Carbonic anhydrase II inhibition. In order to go in deep sight to the selectivity of the benzenesulfonamides derivatives, CA II enzyme inhibition was carried out to the most potent derivatives **4e**, **4g** and **4h**. The results revealed that the synthesized compounds didn't inhibit the cytosolic CA II which is a required feature for compounds targeting tumor – associated enzymes (Table 2).

3.2.4 Cell cycle analysis. The effect of benzenesulfonamide analogue **4e** on cell cycle progression was performed against MDA-MB-231 breast cancer cell line, *via* a DNA flow cytometric

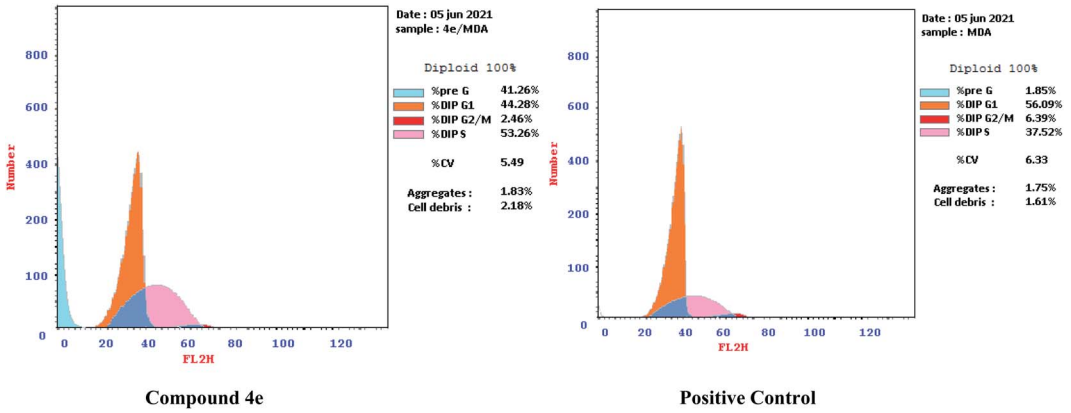

Fig. 6 Effect of compound **4e** on the phases of cell cycle of MDA-MB-231 cell lines.

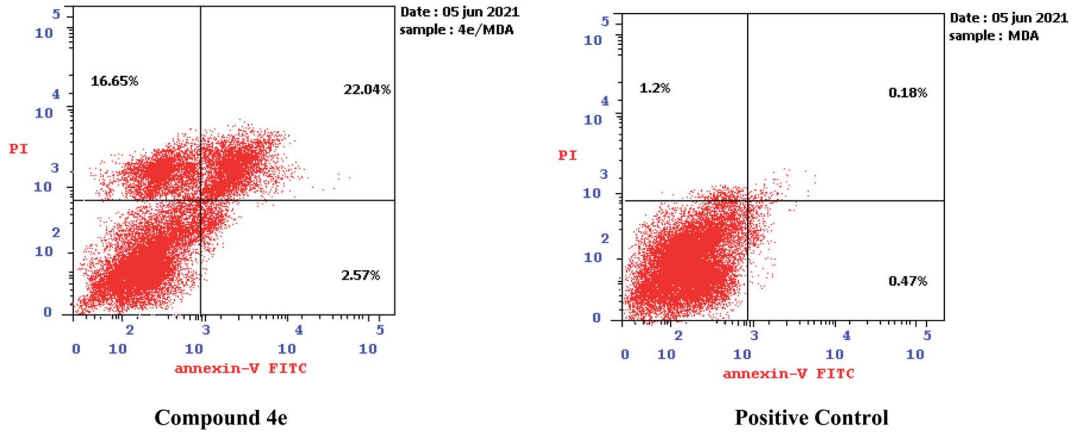

Fig. 7 Effect of compound **4e** on the percentage of annexin V-FITC-positive staining against MDA-MB-231.

assay (Fig. 6). The MDA-MB-231 cells was treated with derivative **4e** at its IC_{50} concentration ($IC_{50} = 3.58$ μM) for 24 h. The results of this flow cytometric assay (Fig. 6) revealed that exposure of MDA-MB-231 cells to compound **4e** led to a remarkable increase in the percentage of cells at pre-G1 by 22 fold, associated with concurrent significant arrest in the S phase by 1.4 fold, compared to positive control. Thus compound **4e** provokes apoptosis by arresting the cell cycle.

3.2.5 Annexin V-FITC apoptosis assay. The cytotoxic activity of thiazolone–benzenesulfonamide **4e** was examined for its consistency to induce apoptosis against MDA-MB-231 cancer cells, so Annexin V-FITC/propidium iodide assay was performed *via* flow cytometry (Fig. 7).

The outcomes showed that compound **4e** had the ability to induce apoptosis against MDA-MB-231 cells that is evidenced by the considerable increase in the percent of annexin V-FITC-positive apoptotic cells, appearing in the late apoptotic phase (from 0.18% to 22.04%) in addition to necrosis phase (from 1.20% to 16.65%), which signifies about 22 fold total increase when compared to positive control.

3.2.6 Antimicrobial activity. Thiazolidinone–benzene sulfonamide compounds have been identified as attractive scaffolds for the innovation of new antibacterial agents, based on earlier reports on their antibacterial ability.[48] Therefore, all the synthesized compounds (**4a–j**) were evaluated against *K. pneumonia*, *E. coli*, *P. vulgaris*, *S. aureus*, *S. typhimurium*, *P. aeruginosa* and *C. albicans* (Table 3). The antimicrobial results revealed that synthesized compound **4d** (chloro analogue) displayed moderate antimicrobial activity against *K. pneumonia*, *S. aureus* and *S. typhimurium* with growth inhibition of 59.28%, 72.62% and 64.68%, respectively comparing with ciprofloxacin as positive control with growth inhibition of 99.7%, 99.25% and 99.56% respectively. Eugenol analogue **4e** exhibited the most potent antibacterial activity among the synthesized derivatives against *S. aureus* and *S. typhimurium* with growth inhibition 80.69% and 75.09% respectively. This is in addition to its considerable antibacterial activity against *K. pneumonia*, and *E.*

Table 3 Antimicrobial activity in inhibition ratio for the synthesized compounds

Test microbes[a] (inhibition ratio%)							
Compound no.	*K. pneumonia*	*E. coli*	*P. vulgaris*	*S. aureus*	*S. typhimurium*	*P. aeruginosa*	*C. albicans*
4a	NA	NA	NA	NA	NA	15.33	NA
4b	NA	NA	NA	NA	NA	18.61	8.87
4c	14.43	25.68	0.00	15.58	NA	27.37	NA
4d	**59.28**	NA	33.47	**72.62**	**64.68**	40.88	NA
4e	**62.89**	**60.66**	41.95	**80.69**	**75.09**	32.12	NA
4f	26.80	46.45	3.39	57.93	45.72	NA	NA
4g	NA	NA	23.31	**69.74**	**60.97**	**73.36**	NA
4h	33.51	29.51	19.07	**68.30**	**59.11**	27.01	NA
4i	NA	NA	NA	NA	NA	NA	NA
4j	NA	NA	5.08	NA	NA	37.59	NA
Cip	99.7	99.1	99.78	99.25	99.56	99.25	—
Nys	—	—	—	—	—	—	99.21

[a] Cip: ciprofloxacin, Nys: nystatin, NA: not active.

Table 4 Anti-biofilm activity of synthesized compounds **4a–j** at 50 μg mL^{-1} against different bacterial strains

Biofilm inhibition ratio%						
Compound no.	*K. pneumonia*	*E. coli*	*P. vulgaris*	*S. aureus*	*S. typhimurium*	*P. aeruginosa*
4a	NA	NA	16.30	NA	NA	NA
4b	**78.29**	18.78	16.85	**53.06**	NA	45.51
4c	**54.26**	NA	NA	NA	NA	NA
4d	NA	NA	NA	NA	NA	NA
4e	18.60	15.47	**61.41**	45.92	**63.43**	NA
4f	10.08	19.89	**64.67**	21.43	36.57	NA
4g	**79.46**	NA	NA	35.24	NA	NA
4h	**77.52**	19.89	50.54	19.39	**66.86**	35.96
4i	5.43	49.72	7.61	22.55	22.86	NA
4j	NA	NA	NA	NA	NA	NA

coli with growth inhibition of 62.89%, and 60.66%, respectively (Table 3). Furthermore, a significant inhibitory effect was displayed to compound **4g** against *S. aureus*, *S. typhimurium*, and *P. aeruginosa* with inhibitory effect 69.74%, 60.97% and 73.36% respectively when compared to ciprofloxacin. Finally, the vanillin analogue **4h** showed moderate growth inhibition against *S. aureus* and *S. typhimurium via* 68.30% and 59.11% respectively when compared to ciprofloxacin (Table 3). Based on these results presence of electron withdrawing groups (as Cl and NO_2) on aryl moiety improved the antibacterial activity of the synthesized compounds against *S. aureus*, and *S. typhimurium*. Also, the poly substitution on the aryl ring enhanced the antibacterial activity against *S. aureus*, *S. typhimurium*, *K. pneumonia* and *E. coli*.

3.2.7 Anti-biofilm activity. In order to further determine the inhibitory activity of the synthesized compounds (**4a–j**),

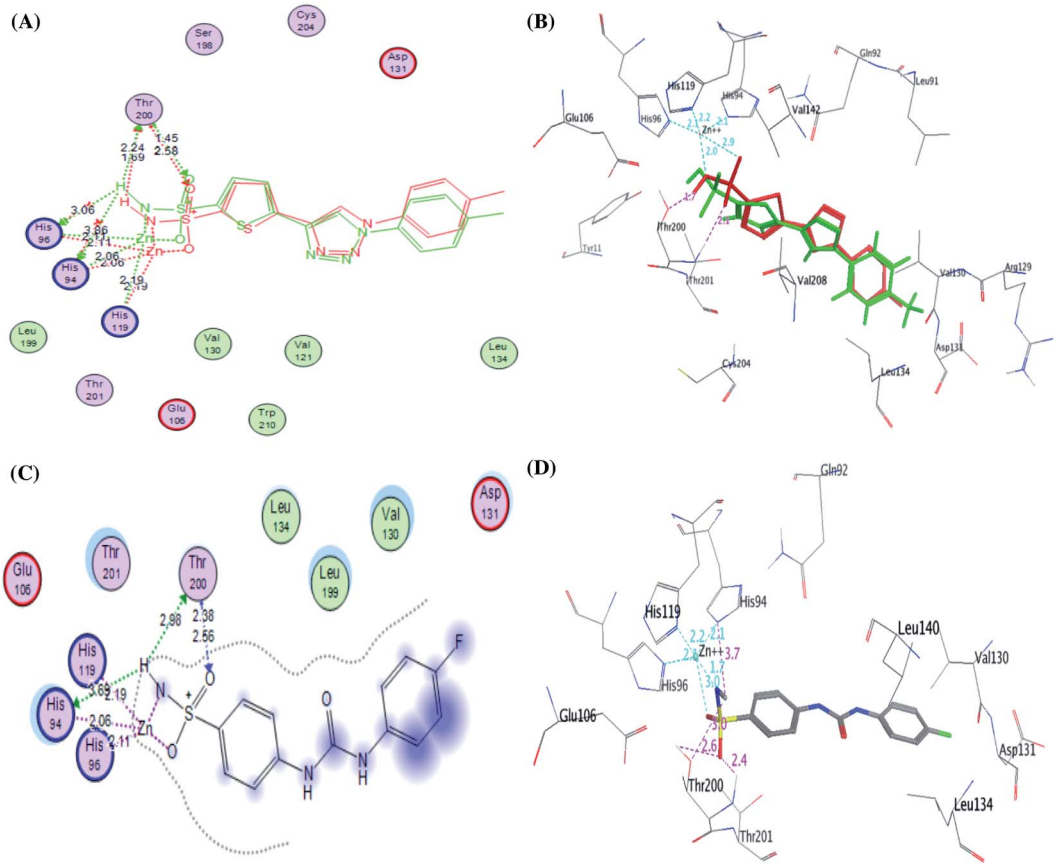

Fig. 8 2D diagram (A) and 3D diagram (B) of the superimposed of the co-crystallized (red) and the docking pose (blue) of native ligand within active site of CA IX with RMSD of 1.41 Å. In addition, 2D diagram (C) and 3D representation (D) of compound **SLC-0111** within the CA IX binding site.

their antibiofilm potentials against *K. pneumonia*, *E. coli*, *P. vulgaris*, *S. aureus*, *S. typhimurium*, and *P. aeruginosa* were determined. Compounds **4b** and **4c** displayed significant antibiofilm activity against *K. pneumonia* with % inhibition rates of 78.29% and 54.26%, respectively. Interestingly, both carbonic anhydrase IX inhibitors **4g** and **4h** exhibited excellent inhibitory activity against *K. pneumonia* with % inhibition of 79.46% and 77.52% respectively. In addition to its inhibitory effect against *K. pneumonia*, the vanillin derivative **4h** exhibited 66.86% inhibition against *S. typhimurium*. The eugenol derivative **4e** showed potent inhibitory activity against *P. vulgaris*, and *S. typhimurium* with % inhibition rates of 61.41% and 63.43%, respectively (Table 4). Moreover, the carboxylic acid analogue **4f** revealed significant inhibitory activity against *P. vulgaris* with 64.67% inhibition. From these results, it could be concluded that presence of electron donating group enhanced the antibiofilm effect towards Gram negative bacteria as *K. pneumonia*. Moreover, the poly substitution on the aryl ring (**4e** and **4h**) enhanced the antibiofilm effect toward *S. typhimurium*.

3.2.8 Molecular docking studies. This study was conducted to identify the activity of the newly synthesized benzenesulfonamide derivatives and to understand some structural observations for their binding modes and their binding interactions with CA IX enzyme. Consequently, the most active derivatives (**4e**, **4g** and **4h**) in addition to compound **4f**, as a representative for the least active compounds for comparison, were docked within the active site of CA IX using Molecular Operating Environment (MOE, 2010.10) software. The 3D crystal structure of CA IX (PDB ID: 5FL6) in complex with 5-(1-(4-methylphenyl)-1*H*-1,2,3-triazol-4-yl)thiophene-2-sulfonamide was used for this docking study.[49,50] First, the docking setup was validated by performing redocking of the co-crystalized ligand in the CA IX binding site. The redocking validation step of the co-crystallized ligand accurately indicates that the utilized docking protocol is appropriate for this current docking simulation. This is demonstrated by the small RMSD value between the redocked pose and the co-crystallized ligand (1.41 Å); the energy binding score (S) = −9.1411 kcal mol^{-1} and the ability of the docked pose to occupy all the key interactions achieved by the co-crystallized ligand with the CA IX active site hot spots (Fig. 8). Accordingly, the validation process used in anticipating the ligand-target interactions at the binding site for the compounds was successful. It is worth to mention that **SLC-0111** was docked in the binding site of the CA IX and it exhibited the same binding interactions as the native ligand (Fig. 8).

The CA IX catalytic pocket is reportedly as cone-shaped cavity, which is segregated into two characteristic conserved environments as mentioned before. So, docking results of the active analogues **4e**, **4g** and **4h** suggested that they all fit accurately within the active site involving some interactions including coordination bonds and hydrogen bonds. Generally, it was recognized that the top docked poses have a common binding configuration and orientation that the phenyl-bearing sulfonamide moiety in the mentioned derivatives aligned towards His94, His96, His119, Thr200, Thr201, Tyr11 and Glu106 amino acids residues while the benzylidene moieties were extended towards Arg129, Val130, Asp131 and Leu134 residues forming some H bond interactions. Their remarkable potency against CA IX enzyme may be significantly due to the apparent similarity between the predicted binding patterns of these analogues and **SLC-0111**, the results of the docking studies are represented in Table 5.

It was conceptualized that the type and number of these interactions could explain the variation between these ligands in their potency. The most active predicted eugenol derivative **4e** (IC_{50} = 10.93 ± 0.53 nM) exhibited the highest number and types of interactions. It formed five different H-bonds; two H-bonds between the hydroxyl and methoxy groups of eugenol moiety and Asp131, one H-bond between NH group of sulphonamide and His94, two H-bonds between oxygen group of sulphonamide and Thr200. Furthermore, the sulfonamide group showed coordination bonds with Zn^{2+} ion and three histidine residues (His94, His96, and His119) as shown in Fig. 9A and B.

Table 5 Docking energy scores (S) in kcal mol^{-1}, interacting amino acid, distance in Å of the tested compounds **4e**, **4f**, **4g**, **4h** and **SLC-0111**

Cpd no.	S score[a] kcal mol^{-1}	Amino acid/bond	Distance (Å)
4e	−15.5765	His94/Zn-coordination bond	2.06
		His96/Zn-coordination bond	2.11
		His119/Zn-coordination bond	2.19
		His94/H-donor	2.49
		Thr200/H-acceptor	2.07
		Thr200/H-acceptor	3.16
		Asp131/H-donor	2.11
		Asp131/H-acceptor	2.46
4f	−9.5118	His94/Zn-coordination bond	2.06
		His96/Zn-coordination bond	2.11
		His119/Zn-coordination bond	2.19
4g	−12.4361	His94/Zn-coordination bond	2.06
		His96/Zn-coordination bond	2.11
		His119/Zn-coordination bond	2.19
		His96/H-acceptor	3.03
		Thr200/H-acceptor	2.29
		Thr200/H-acceptor	2.63
		Gln71/H-acceptor	1.71
4h	−10.5835	His94/Zn-coordination bond	2.06
		His96/Zn-coordination bond	2.11
		His119/Zn-coordination bond	2.19
		Thr200/H-donor	2.07
		Thr200/H-acceptor	2.47
		Asp131/H-acceptor	3.75
SLC-0111	−11.0025	His94/Zn-coordination bond	2.06
		His96/Zn-coordination bond	2.11
		His119/Zn-coordination bond	2.19
		His94/H-donor	2.69
		Thr200/H-donor	2.98
		Thr200/H-acceptor	2.38
		Thr200/H-acceptor	2.56

[a] S: the score of placement of a compound into the binding pocket of protein using London dG scoring function.

Compared to eugenol derivative **4e**, the decreased inhibition of *p*-nitrobenzylidene derivative **4g** against CA IX (IC_{50} = 16.96 ± 0.83 nM) could be explained by the absence of some interactions such as two H-bonds with Asp131 indicating that the replacement of the EDG (OCH_3 and OH) with EWG (P-NO_2) resulted in the absence of an important H-bond with Asp131 amino acid in the active site of CA IX enzyme, on the other side, carbonyl group of thiazol-4-one moiety showed H-bond with Gln71 (Fig. 9C and D). However, 4-hydroxy-3-methoxybenzylidene derivative **4h** showed the least activity (IC_{50} = 25.56 ± 1.25 nM) between the most active ones due to the reduction in the number of interactions despite of adopting a similar orientation (Fig. 9E and F).

Furthermore, the exploration of the docking outcomes of the least active compound **4f** into the CA IX active pocket indicated that compound **4f** possessed a totally opposing orientation and dispositioning compared with the previously docked active compounds (**4e**, **4g** and **4h**) as shown in Fig. 10. It was found

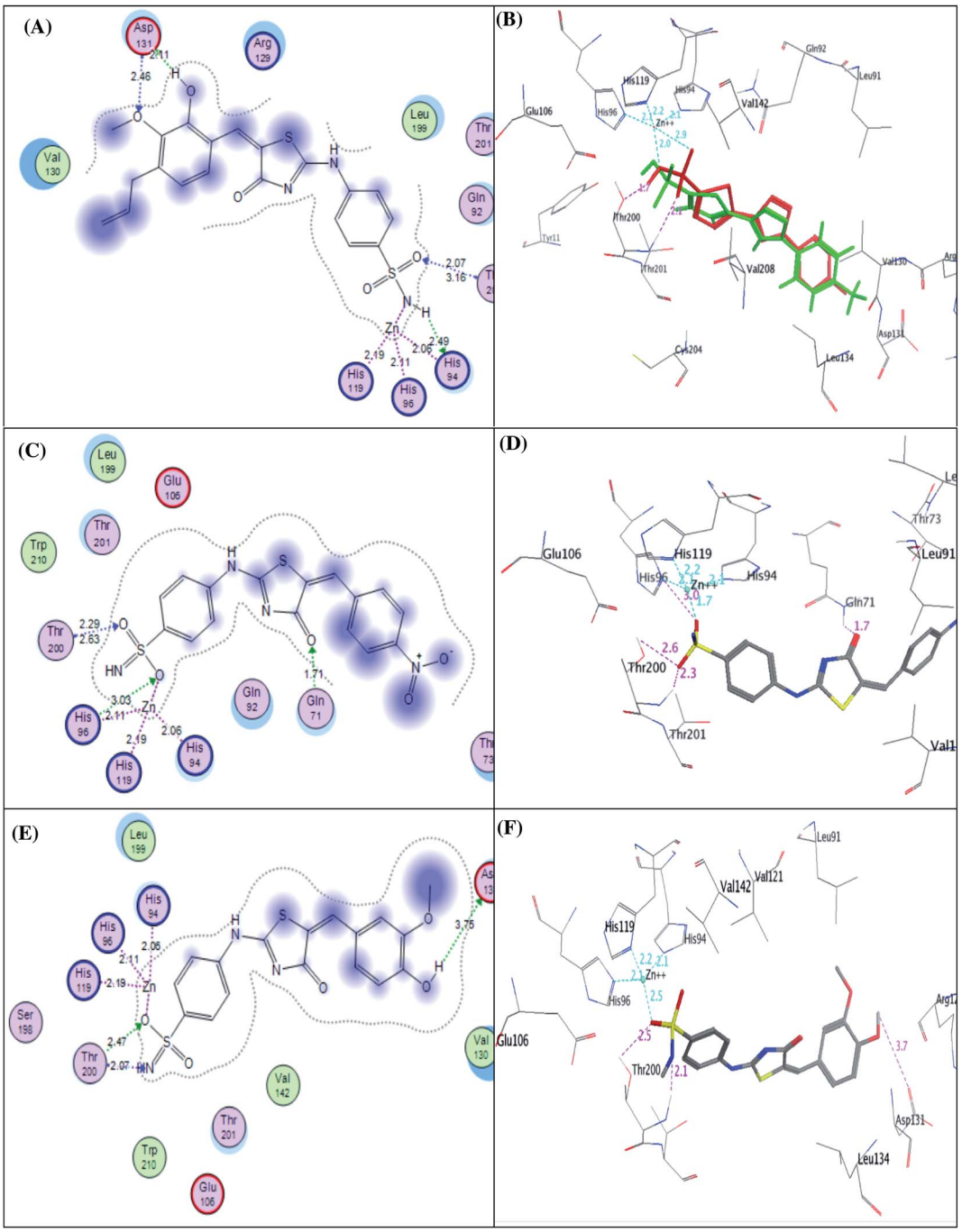

Fig. 9 2D diagram (A) and 3D pose (B) of compound **4e**, 2D diagram (C) and 3D pose (D) of compound **4g**, and 2D diagram (E) and 3D pose (F) of compound **4h** within binding site of CA IX binding site.

that the benzoic acid group was located near His94, His96, His119, Thr200, Thr201, Tyr11 and Glu106 residues and exhibited coordination bonds with Zn^{2+} ion and three histidine residues (His94, His96, and His119), while the benzenesulfonamide core was extended towards Arg129, Val130, Asp131 and Leu134 residues and don't exhibited any interactions mirrored in a decrease in the CA IX inhibitory activity. As a result, docking study was coherent with the *in vitro* assay results, verifying that hybridization between the phenyl-bearing sulfonamide pharmacophoric and the thiazole-4-one CA IX moieties are promising leads for further optimization.

3.2.9 Prediction of ADMET properties. In the current study, the pharmacokinetic properties predicted to the mostly potent CAIX inhibitors (**4e**, **4g** and **4h**) were assessed. These molecular predictions of the mentioned derivatives depending on the computed partition coefficient (log *P*) revealed that all the studied analogues had a good lipophilicity as their log *P* values were less than 5 (ref. 51) (Table S2†). The predicted lipophilicities are negatively associated with their water solubility potentials but have a correlation with caco-2 permeability. Absorption is a very complex process that is defined as movement of a drug from an extravascular site of administration into the systemic circulation depending on permeability and solubility of the compound.[52] For oral drugs, absorption occurs by either transcellular diffusion, paracellular diffusion, and transporter-mediated mechanisms and caco-2 cell lines[53] was used to estimate the latter mechanism. Lagorce *et al.*[54] reported that enzyme inhibitors showed lower caco-2 permeability than ion channels and nuclear receptors. Thus, this may explain the low absorption properties of the examined compounds. Furthermore, caco-2 permeability and human intestinal absorption have a role in determining the bioavailability of the drugs. From the results represented, all the examined derivatives illustrated an elevated cellular permeability prediction, particularly compound **4g** that displayed 81.72% intestinal absorption (Table S2†). Skin permeability is a crucial consideration for the development of transdermal drug delivery. All the synthesized compounds showed good skin permeability. The three derivatives were found to be substrate of *P*-glycoprotein. Yet, neither of the evaluated derivatives were expected as *P*-glycoprotein II inhibitors. Additionally, the distribution of drug refers to its distribution throughout the body. Some parameters were investigated *in silico* regarding distribution that include blood brain barrier (BBB) permeability, and central nervous system (CNS) permeability. Also, the free (unbound) drug is also important to be monitored due to its availability to interact with the protein target.[55] Prediction of distribution descriptors revealed that the synthesized analogues showed desirable theoretical dose related to uniform plasma distribution. Moreover, all the estimated benzenesulfonamides based derivatives expressed poor brain distribution but are capable of penetrating CNS (Table S2†). In the same context, metabolism is the biotransformation of the drug to facilitate tis excretion. Thus, metabolism prediction showed that all synthesized analogues showed low CYP promiscuity, however compound **4e** can inhibit CYP2C19 and CYP2C9 while **4g** analogue inhibit CYP3A4, however all compounds are CYP3A4 substrate. These findings indicated that the mentioned derivatives could have a role in drug–drug interactions and oxidative stress could be initiated. Analogue **4h** is expected to be a Renal OCT2 substrate with respect to excretion prediction. Finally, toxicological predictions of the synthesized analogues were estimated using pkCSM software. Herein, *via* AMES toxicity testing, the bacterial mutagenic ability of the benzenesulfonamide derivatives showed that all analogues could be regarded as non-mutagenic agents. Nevertheless, the toxicity of all the analogues in *T. pyriformis* are high.

Moreover, one of the significant parameters of toxicity, which is cardiotoxicity, was predicted for the investigated compounds; human ether-a-go-go-go-related gene I, II (hERG I, II). The predicted outcomes presented that the estimated compuds didn't inhibit hERG I, II, except for vanillin derivative

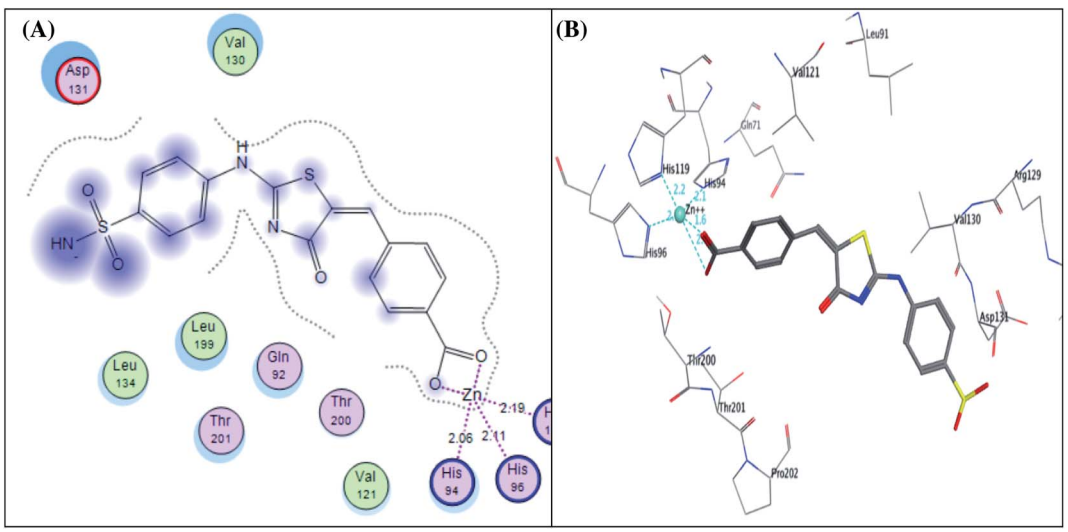

Fig. 10 2D diagram (A) and 3D pose (B) of compound **4f** within the binding site of CA IX.

4e that inhibits hERG II, that may reflect normal cardiac rhythm.

4 Conclusion

In this work, a new series of sulfonamide derivatives containing thiazolone ring with different aryl moieties were designed and synthesized as potent carbonic anhydrase IX inhibitors. The synthesized derivatives were evaluated for their anticancer activity against two human BC cell lines (MDA-MB-231 and MCF-7) in addition to normal human cell line (MCF-10A). All the compounds were evaluated for their inhibitory activity against CA IX in a range with 10.93–25.06 nM. Three analogues **4e**, **4g** and **4h** displayed significant selectivity towards tumor assisted CA IX over cytosolic CA II. From the results, we can conclude that the introduction of eugenol aldehyde or vanillin moieties (electron donating groups) are associated with enhanced anticancer activity (IC_{50} = 3.58 and 1.56 μM) against MDA-MB-231 and (IC_{50} = 4.58 and 1.52 μM) against MCF-7 as well as remarkable selectivity over normal breast cell line MCF-10A. This can be explained in accordance to docking studies due to their high binding affinities *via* forming high number and types of interactions. Additionally, compound **4e** was able to induce apoptosis in MDA-MB-231 cells confirmed by the increase of annexinV – FITC percent by 22 fold. Moreover, the synthesized analogues were screened against antibacterial and anti-biofilm inhibition. The presence of electron withdrawing groups (as Cl and NO_2) on the aryl moiety was shown to improve the antibacterial activity against *S. aureus*, and *S. typhimurium* while the presence of electron donating group enhanced the anti-biofilm effect towards Gram negative bacteria as *K. pneumonia*. Moreover, the poly substitution on the aryl ring (**4e** and **4h**) enhanced the antibiofilm effect toward *S. typhimurium*.

Compliance with ethical standards

Research involving human participants and/or animals

This work did not use human volunteers or animals.

Ethics approval and consent to participate

Not applicable.

Funding

This work is self-funded.

Conflicts of interest

Authors declare that they have no conflict of interest.

Acknowledgements

The authors express their appreciation and thanks to Dr Mohamed Abdel-Mohsen Elzayat, pharmacology department, NUB University to his kind assistance in performing ANOVA statistical analysis.

References

1 A. Kamal, K. S. Reddy, M. N. A. Khan, R. V. C. Shetti, M. J. Ramaiah, S. N. Pushpavalli, C. Srinivas, M. P. Bhadra, M. Chourasia, G. N. Sastry, A. Juvekar, S. Zingde and M. Barkume, Synthesis, DNA-binding ability and anticancer activity of benzothiazole/benzoxazole–pyrrolo [2,1-*c*][1,4]benzodiazepine conjugates, *Bioorg. Med. Chem.*, 2010, **18**, 4747–4761.

2 D. Verma, P. Kumar, B. Narasimhan, K. Ramasamy, V. Mani, R. K. Mishra and A. B. Abdul Majeed, Synthesis, antimicrobial, anticancer and QSAR studies of 1-[4-(substituted phenyl)-2-(substituted phenyl azomethyl)-benzo[*b*]-[1,4]diazepin-1-yl]-2-substituted phenylaminoethanones, *Arabian J. Chem.*, 2019, **12**, 2882–2896.

3 M. T. M. Nemr and A. M. AboulMagd, New fused pyrimidine derivatives with anticancer activity: synthesis, topoisomerase II inhibition, apoptotic inducing activity and molecular modeling study, *Bioorg. Chem.*, 2020, **103**, 104134.

4 M. T. M. Nemr, A. Sonousi and A. A. Marzouk, Design, synthesis and antiproliferative evaluation of new tricyclic fused thiazolopyrimidines targeting topoisomerase II: molecular docking and apoptosis inducing activity, *Bioorg. Chem.*, 2020, **105**, 104446.

5 https://www.uicc.org/news/globocan-2020-new-global-cancer-data.

6 K. Ruan, G. Song and G. Ouyang, Role of hypoxia in the hallmarks of human cancer, *J. Cell. Biochem.*, 2009, **107**, 1053–1062.

7 J. P. Cosse and C. Michiels, Tumour hypoxia affects the responsiveness of cancer cells to chemotherapy and promotes cancer progression, *Adv. Anticancer Agents Med. Chem.*, 2008, **8**, 790–797.

8 U. Lendahl, K. L. Lee, H. Yang and L. Poellinger, Generating specificity and diversity in the transcriptional response to hypoxia, *Nat. Rev. Genet.*, 2009, **10**, 821–832.

9 A. Güttler, K. Theuerkorn, A. Riemann, H. Wichmann, J. Kessler, O. Thews, M. Bache and D. Vordermark, Cellular and radiobiological effects of carbonic anhydrase IX in human breast cancer cells, *Oncol. Rep.*, 2019, **41**, 2585–2594.

10 C. T. Supuran, Structure-based drug discovery of carbonic anhydrase inhibitors, *J. Enzyme Inhib. Med. Chem.*, 2012, **27**, 759–772.

11 C. T. Supuran, How many carbonic anhydrase inhibition mechanisms exist?, *J. Enzyme Inhib. Med. Chem.*, 2016, **31**, 345–360.

12 J. R. Casey, P. E. Morgan, D. Vullo, A. Scozzafava, A. Mastrolorenzo and C. T. Supuran, Carbonic anhydrase inhibitors. Design of selective, membrane-impermeant inhibitors targeting the human tumor-associated isozyme IX, *J. Med. Chem.*, 2004, **47**, 2337–2347.

13 V. Alterio, A. Di Fiore, K. D'Ambrosio, C. T. Supuran and G. D. Simone, Multiple binding modes of inhibitors to carbonic anhydrases: how to design specific drugs

targeting 15 different isoforms?, *Chem. Rev.*, 2012, **112**, 4421–4468.

14 E. Rosatelli, A. Carotti, M. Ceruso, C. T. Supuran and A. Gioiello, Flow synthesis and biological activity of aryl sulfonamides as selective carbonic anhydrase IX and XII inhibitors, *Bioorg. Med. Chem. Lett.*, 2014, **24**, 3422–3425.

15 B. P. Mahon, M. A. Pinard and R. McKenna, Targeting carbonic anhydrase IX activity and expression, *Molecules*, 2015, **20**, 2323–2348.

16 N. Chandak, M. Ceruso, T. C. Supuran and K. P. Sharma, Novel sulfonamide bearing coumarin scaffolds as selective inhibitors of tumor associated carbonic anhydrase isoforms IX and XII, *Bioorg. Med. Chem.*, 2016, **2**, 2882–2886.

17 M. A. Abdelrahman, W. M. Eldehna, A. Nocentini, S. Bua, S. T. Al-Rashood, G. S. Hassan, A. Bonardi, A. A. Almehizia, H. M. Alkahtani, A. Alharbi, P. Gratteri and C. T. Supuran, Novel Diamide-Based Benzenesulfonamides as Selective Carbonic Anhydrase IX Inhibitors Endowed with Antitumor Activity: Synthesis, Biological Evaluation and *In Silico* Insights, *Int. J. Mol. Sci.*, 2019, **20**, 2484.

18 N. M. Abdel Gawad, N. H. Amin, M. T. Elsaadi, F. M. M. Mohamed, A. Angeli, V. D. Luca, C. Capasso and C. T. Supuran, Synthesis of 4-(thiazol-2-ylamino)-benzenesulfonamides with carbonic anhydrase I, II and IX inhibitory activity and cytotoxic effects against breast cancer cell lines, *Bioorg. Med. Chem.*, 2016, **24**, 3043–3051.

19 A. Grandane, M. Tanc, L. D. Mannelli, F. Carta, C. Ghelardini, R. Žalubovskis and C. T. Supuran, 6-Substituted sulfocoumarins are selective carbonic anhdydrase IX and XII inhibitors with significant cytotoxicity against colorectal cancer cells, *J. Med. Chem.*, 2015, **58**, 3975–3983.

20 E. Andreucci, J. Ruzzolini, S. Peppicelli, F. Bianchini, A. Laurenzana, F. Carta, C. T. Supuran and L. Calorini, The carbonic anhydrase IX inhibitor SLC-0111 sensitises cancer cells to conventional chemotherapy, *J. Enzyme Inhib. Med. Chem.*, 2019, **34**, 117–123.

21 A. Insuasty, J. Ramírez, M. Raimondi, C. Echeverry, J. Quiroga, R. Abonia, M. Nogueras, J. Cobo, M. V. Rodrígue, S. A. Zacchino and B. Insuasty, Synthesis, antifungal and antitumor activity of novel (*Z*)-5-hetarylmethylidene-1,3-thiazol-4-ones and (*Z*)-5-ethylidene-1,3-thiazol-4-ones, *Molecules*, 2013, **18**, 5482–5497.

22 D. Havrylyuk, B. Zimenkovsky, O. Vasylenko, L. Zaprutko, A. Gzella and R. Lesyk, Synthesis of novel thiazolone-based compounds containing pyrazoline moiety and evaluation of their anticancer activity, *Eur. J. Med. Chem.*, 2009, **44**, 1396–1404.

23 P. Vicini, A. Geronikaki, K. Anastasia, M. Incerti and F. Zani, Synthesis and antimicrobial activity of novel 2-thiazolylimino-5-arylidene-4-thiazolidinones, *Bioorg. Med. Chem.*, 2006, **14**, 3859–3864.

24 N. A. Khalil, E. M. Ahmed and H. B. El-Nassan, Synthesis, characterization, and biological evaluation of certain 1,3-thiazolone derivatives bearing pyrazoline moiety as potential anti-breast cancer agents, *Med. Chem. Res.*, 2013, **22**, 1021–1027.

25 G. Turan-Zitouni, L. Yurttas, A. Tabbi, G. A. Çiftçi, H. E. Temel and Z. A. Kaplancıklı, New Thiazoline-Tetralin Derivatives and Biological Activity Evaluation, *Molecules*, 2018, **23**, 135.

26 G. N. Masoud, A. M. Youssef, M. M. Abdel Khalek, A. E. Abdel Wahab, I. M. Labouta and A. A. B. Hazzaa, Design, synthesis, and biological evaluation of new 4-thiazolidinone derivatives substituted with benzimidazole ring as potential chemotherapeutic agents, *Med. Chem. Res.*, 2013, **22**, 707–725.

27 J. Wu, L. Yu, F. Yang, J. Li, P. Wang, W. Zhou, L. Qin, Y. Li, J. Luo, Z. Yi, M. Liu and Y. Chen, Optimization of 2-(3-(arylalkyl amino carbonyl)phenyl)-3-(2-methoxyphenyl)-4-thiazolidinone derivatives as potent antitumor growth and metastasis agents, *Eur. J. Med. Chem.*, 2014, **80**, 340–351.

28 C. T. Supuran, Carbonic anhydrase inhibitors and their potential in a range of therapeutic areas, *Expert Opin. Ther. Pat.*, 2018, **28**, 709–712.

29 C. T. Supuran, Applications of carbonic anhydrases inhibitors in renal and central nervous system diseases, *Expert Opin. Ther. Pat.*, 2018, **28**, 713–721.

30 C. T. Supuran, How many carbonic anhydrase inhibition mechanisms exist?, *J. Enzyme Inhib. Med. Chem.*, 2015, **31**, 345–360.

31 T. V. Wani, S. Bua, P. S. Khude, A. H. Chowdhary, C. T. Supuran and M. P. Toraskar, Evaluation of sulphonamide derivatives acting as inhibitors of human carbonic anhydrase isoforms I, II and Mycobacterium tuberculosis b-class enzyme Rv3273, *J. Enzyme Inhib. Med. Chem.*, 2018, **33**, 962–971.

32 S. G. Alegaon and K. R. Alagawadi, New thiazolidinedione-5-acetic acid amide derivatives: synthesis, characterization and investigation of antimicrobial and cytotoxic properties, *Med. Chem. Res.*, 2012, **21**, 816–824.

33 H. Z. Chohan, U. A. Shaikh, A. Rauf and T. C. Supuran, Antibacterial, antifungal and cytotoxic properties of novel N-substituted sulfonamides from 4-hydroxycoumarin, *J. Enzyme Inhib. Med. Chem.*, 2006, **21**, 741–748.

34 M. D. Altıntop, Z. A. Kaplancıklı, G. A. Çiftçi and R. Demirel, Synthesis and biological evaluation of thiazoline derivatives as new antimicrobial and anticancer agents, *Eur. J. Med. Chem.*, 2014, **74**, 264–277.

35 A. M. Alafeefy, M. Ceruso, A. S. Al-Tamimi, S. Del Prete, C. Capasso and C. T. Supuran, Quinazoline–sulfonamides with potent inhibitory activity against the α-carbonic anhydrase from Vibrio cholerae, *Bioorg. Med. Chem.*, 2014, **22**, 5133–5140.

36 K. O. Mohamed, Y. M. Nissan, A. A. El-Malah, W. A. Ahmed, D. M. Ibrahim, T. M. Sakr and M. A. Motaleb, Design, synthesis and biological evaluation of some novel sulfonamide derivatives as apoptosis inducers, *Eur. J. Med. Chem.*, 2017, **135**, 424–433.

37 Y. M. Nissan, K. O. Mohamed, W. A. Ahmed, D. M. Ibrahim, M. M. Sharaky, T. M. Sakr, M. A. Motaleb, A. Maher and R. K. Arafa, New benzenesulfonamide scaffold-based cytotoxic agents: design, synthesis, cell viability, apoptotic

activity and radioactive tracing studies, *Bioorg. Chem.*, 2020, **96**, 103577.

38 D. T. Vistica, P. Skehan, D. Scudiero, A. Monks, A. Pittman and M. R. Boyd, Tetrazolium-based assays for cellular viability: a critical examination of selected parameters affecting formazan production, *Cancer Res.*, 1991, **51**, 2515–2520.

39 H. Takeuchi, M. Baba and S. Shigeta, An application of tetrazolium (MTT) colorimetric assay for the screening of anti-herpes simplex virus compounds, *J. Virol. Methods*, 1991, **33**, 61–71.

40 W. M. Eldehna, D. H. El-Naggar, A. R. Hamed, H. S. Ibrahim, H. A. Ghabbour, H. A. Abdel-Aziz and H. A. Ghabbour, One-pot three-component synthesis of novel spirooxindoles with potential cytotoxic activity against triple-negative breast cancer MDAMB-231 cells, *J. Enzyme Inhib. Med. Chem.*, 2018, **33**, 309–318.

41 W. M. Eldehna, H. Almahli, G. H. Al-Ansary, H. A. Ghabbour, M. H. Aly, O. E. Ismael, A. Al-Dhfyan and H. A. Abdel-Aziz, Synthesis and in vitro anti-proliferative activity of some novel isatins conjugated with quinazoline/phthalazine hydrazines against triple-negative breast cancer MDA-MB-231 cells as apoptosis-inducing agents, *J. Enzyme Inhib. Med. Chem.*, 2017, **32**, 600–613.

42 R. A. Ingebrigtsen, E. Hansen, J. H. Andersen and H. C. Eilertsen, Light and temperature effects on bioactivity in diatoms., *J. Appl. Phycol.*, 2016, **28**, 939–950.

43 S. I. Elewa, A. O. Abdelhamid, A. A. Hamed and E. Mansour, Synthesis, characterization, antimicrobial activities, anticancer of some new pyridines from 2, 3-dihydro-2-oxo-4-phenyl-6-(thien-2-yl) pyridine-3-carbonitrile, *Synth. Commun.*, 2021, **51**, 151–161.

44 D. M. Eskander, S. M. M. Atalla, A. A. Hamed and E. D. A. El-Khrisy, Investigation of secondary metabolites and its bioactivity from *Sarocladium kiliense* SDA20 using shrimp shell wastes, *Pharmacogn. J.*, 2020, **12**, 636–644.

45 A. A. Hamed, H. Kabary, M. Khedr and A. N. Emam, Antibiofilm, antimicrobial and cytotoxic activity of extracellular green-synthesized silver nanoparticles by two marine-derived actinomycete, *RSC Adv.*, 2020, **10**, 10361–10367.

46 Pharmacokinetic properties, http://biosig.unimelb.edu.au/pkcsm/prediction.

47 S. Mahboobi, A. Sellmer, H. Hocher, E. Eichhorn, T. Bär, M. Schmidt, T. Maier, J. F. Stadlwieser and T. L. Beckers, [4-(Imidazol-1-yl)thiazol-2-yl]phenylamines. A novel class of highly potent colchicine site binding tubulin inhibitors: synthesis and cytotoxic activity on selected human cancer cell lines, *J. Med. Chem.*, 2006, **49**, 5769–5776.

48 A. M. Alafeefy, R. Ahmad, M. Abdulla, W. M. Eldehna, A. S. Al-Tamimi, H. A. Abdel-Aziz, O. Al-Obaid, F. Carta, A. A. Al-Kahtani and C. T. Supuran, Development of certain new 2-substituted-quinazolin-4-yl-aminobenzenesulfonamide as potential antitumor agents, *Eur. J. Med. Chem.*, 2016, **109**, 247–253.

49 J. Leitans, A. Kazaks, A. Balode, J. Ivanova, R. Zalubovskis, C. T. Supuran and K. Tars, Efficient expression and crystallization system of cancer-associated carbonic anhydrase isoform IX, *J. Med. Chem.*, 2015, **58**, 9004–9009.

50 https://www.rcsb.org/structure/5FL6.

51 C. A. Lipinski, F. Lombardo, B. W. Dominy and P. J. Feeney, Experimental and computational approaches to estimate solubility and permeability in drug discovery and development settings, *Adv. Drug Deliv. Rev.*, 2001, **46**, 3–26.

52 M. P. Gleeson, A. Hersey and S. Hannongbua, In-silico ADME models: a general assessment of their utility in drug discovery applications, *Curr. Top. Med. Chem.*, 2011, **11**, 358–381.

53 M. P. Gleeson, Generation of a set of simple, interpretable ADMET rules of thumb, *J. Med. Chem.*, 2008, **51**, 817–834.

54 D. Lagorce, D. Douguet, M. A. Miteva and B. O. Villoutreix, Computational analysis of calculated physicochemical and ADMET properties of protein-protein interaction inhibitors, *Sci. Rep.*, 2017, **7**, 46277.

55 G. Moroy, V. Y. Martiny, P. Vayer, B. O. Villoutreix and M. A. Miteva, Toward *in silico* structure-based ADMET prediction in drug discovery, *Drug Discovery Today*, 2012, **17**, 44–55.